Basin Research

WILEY

Basin Research IAS EAGE

RESEARCH ARTICLE

Detrital Zircon Records of Meso-Neoproterozoic Strata in the Yan-Liao Rift Zone, North China Craton, and Their Implications of Tectono-Sedimentary Evolution

Chenxing Li[1,2] | Jian Chang[1,2] | Nansheng Qiu[1,2]

[1]State Key Laboratory of Petroleum Resources and Engineering, China University of Petroleum (Beijing), Beijing, China | [2]College of Geoscience, China University of Petroleum (Beijing), Beijing, China

Correspondence: Jian Chang (changjian@cup.edu.cn) | Nansheng Qiu (qiunsh@cup.edu.cn)

Received: 8 November 2024 | **Revised:** 8 October 2025 | **Accepted:** 10 October 2025

Funding: This work was supported by the National Key Research and Development Program of China (Grant 2017YFC0603102).

Keywords: detrital zircon | meso-neoproterozoic | North China carton | paleogeographic evolution | Yan-Liao rift zone

ABSTRACT

The Meso-Neoproterozoic eras witnessed critical transitions in supercontinental cycles that shaped global tectonic regimes and paleogeographic configurations. This study presents LA-ICP-MS zircon U–Pb geochronology analyses of thirteen sandstone samples from the Yan-Liao rift zone along the northern North China Craton (NCC) margin to constrain regional tectonic evolution and basin development. Detrital zircon populations exhibit multiple age clusters, with pre-1800 Ma grains derived from NCC basement terranes and younger populations (< 1.8 Ga) correlating with Mesoproterozoic magmatic events. Systematic younging of Maximum Depositional Age (MDA), determined through robust statistical treatment of the multi-MDA method, reveals spatial–temporal depositional patterns controlled by source-to-sink relationships across the rift system. Provenance analysis demonstrates that evolving rift morphology progressively modified zircon transport mechanisms and age distributions, defining four distinct stages of basin evolution between 1.8 and 0.9 Ga. These evolutionary phases exhibit temporal correlations with global supercontinent cycles—initial rifting phases correspond to Columbia breakup (1.8–1.4 Ga), while later tectonic reorganization aligns with Rodinia assembly (1.4–0.9 Ga). Our integrated approach provides critical constraints on NCC margin evolution during Precambrian supercontinental transitions, offering new insights into cratonic responses to global-scale geodynamic processes.

1 | Introduction

Provenance analysis and geochronological investigation of detrital sediments serve as fundamental tools for reconstructing paleogeographic configurations and deciphering tectonic evolution histories (Fonneland et al. 2004; Weltje and von Eynatten 2004; Vermeesch 2013). These methodologies are particularly critical for resolving supercontinent cyclicity, including assembly, stabilization, and breakup events (Yonkee and Weil 2015; Liu, Zhao, et al. 2020; Li et al. 2019; Zhang et al. 2022). The compositional signatures preserved in ancient sedimentary successions reflect a complex interplay of parent rock characteristics, sediment transport dynamics, basin architecture, and paleoenvironmental conditions (Dickinson et al. 1988; Johnsson 1993). Among detrital minerals, zircon has emerged as a premier tracer for provenance studies due to its exceptional resistance to alteration and capacity to retain geochemical and geochronological fingerprints of source terrains (Garzanti et al. 2014; Horton et al. 2015; Geisler et al. 2003; Kennedy et al. 2003). Detrital zircon U–Pb geochronology has proven indispensable for constraining maximum depositional ages (MDAs) of strata lacking biostratigraphic markers or volcanic interlayers (Garzanti and Andò 2007; Sharman and Malkowski 2020; Coutts et al. 2019; Herriott et al. 2019), while systematic comparisons between

Summary

- Integrated zircon U-Pb geochronology and morphology establish the depositional framework of the Yan-Liao Rift.
- Four distinct stages of basin evolution are defined, controlled by evolving rift morphology.
- These stages temporally correlate with the Columbia breakup and subsequent Rodinia assembly.
- This study deciphers the North China Craton's specific response to global supercontinent cycles.

detrital age spectra and potential source regions enable robust paleogeographic reconstructions (Caracciolo 2020; Liu et al. 2022).

The Yan-Liao rift zone along the northern NCC preserves a Meso-Neoproterozoic stratigraphic succession exceeding 10,000 m in thickness, recording nearly one billion years of cratonic evolution (Wang et al. 2015; Liu, Zhang, et al. 2020; Zhu et al. 2022; Deng et al. 2021). While recent revisions to the regional stratigraphy have incorporated radiometric dates from volcanic interbeds (Li et al. 2013; Pang et al. 2020), significant discrepancies between MDAs derived from detrital zircon youngest peak ages and independent geochronological constraints (such as volcanic zircon ages) highlight persistent methodological challenges in determining the actual depositional age of sedimentary rocks (Wan et al. 2011; Liu et al. 2021). This necessitates a critical evaluation of alternative approaches to improve the reliability of detrital zircon chronostratigraphy. Furthermore, the tectonic significance of multiple regional unconformities within this succession remains debated, with proposed mechanisms ranging from craton-scale uplift to eustatic sea-level fluctuations (He et al. 1994; Kuang et al. 2019).

This study presents new detrital zircon U–Pb geochronological data from Meso-Neoproterozoic strata in the central Yan-Liao rift zone, integrated with existing datasets, to address four key objectives: (1) evaluate the reliability of detrital zircon MDAs in temporal calibration of Proterozoic successions; (2) identify spatial variations in sediment provenance through the rift evolution; (3) develop a paleogeographic model reconciling provenance variations with basin dynamics; and (4) elucidate linkages between regional tectonism and supercontinent-scale processes. Our findings advance understanding of Proterozoic stratigraphic architecture, cratonic basin evolution, and Precambrian palaeogeography while proposing an integrated framework for detrital zircon applications in tectonostratigraphic analysis.

2 | Geological Background and Sampling

The NCC, among Earth's oldest Archean cratons, preserves a multi-stage tectonic evolution spanning from the Archean to Phanerozoic (Figure 1a) (Zhai et al. 2003; Zhao et al. 2005; Kusky et al. 2007; Zheng et al. 2013). Bounded by the Qilian Orogen to the west, the Central Asian Orogenic Belt to the north, the Qinling-Dabie Orogen to the south, and the Sulu Ultra-High Pressure Metamorphic Belt to the east (Figure 1b), the NCC formed through the amalgamation of Archean micro blocks, culminating in the collision of the Eastern and Western Blocks along the Trans-North China Orogen (TNCO) at ~1.85 Ga (Zhao et al. 2005; Santosh et al. 2020). Post-collisional extension (~1.85–1.6 Ga) triggered the development of three major Paleoproterozoic rifts, including the Yan-Liao rift zone along the northern NCC margin (Zhai and Liu 2003; Peng et al. 2008). This extensional phase is evidenced by widespread magmatism, such as the Xiong'er Group volcanics (1.8–1.65 Ga), mafic dyke swarms (1.78–1.62 Ga), and anorthosite-rapakivi granite complexes (~1.7 Ga) (Lu et al. 2003; Hou et al. 2008; Yang et al. 2005), which facilitated the deposition of Meso-Neoproterozoic sedimentary successions across the stabilized cratonic basement.

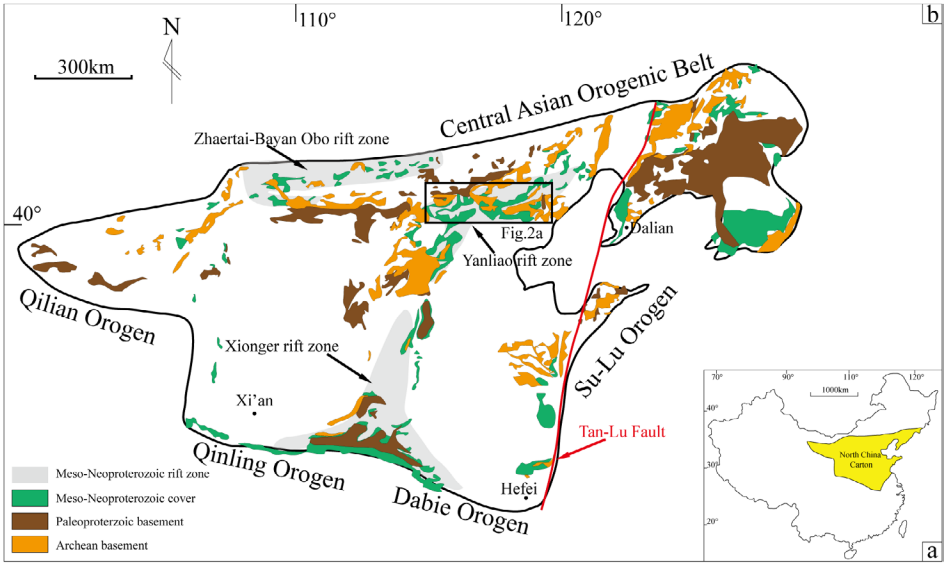

FIGURE 1 | (a) Location of the North China Craton. (b) Archean–Palaeoproterozoic basement and late Palaeoproterozoic to early Neoproterozoic sedimentary cover of the North China Craton (modified after Peng et al. 2011).

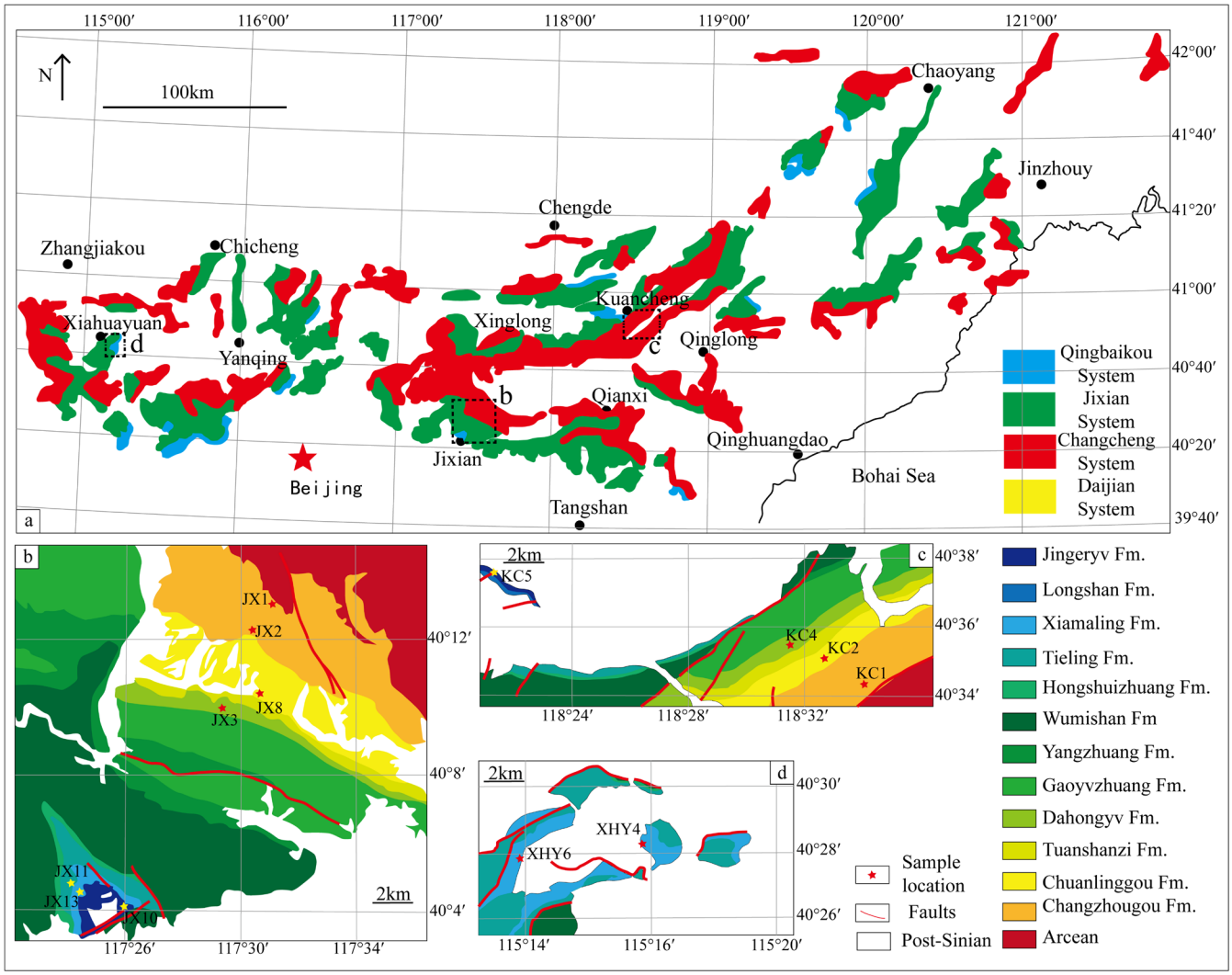

FIGURE 2 | Simplified geological map of the Meso-Neoproterozoic successions in Yan-Liao rift zone (a) (modified after Zhang et al. 2015), Jixian area (b), Kuancheng area (c), and Xiahuayuan area (d), and locations of the detrital zircon samples.

The Yan-Liao rift zone, a prominent intracontinental rift basin along the northern NCC (Figures 1b and 2), hosts a ~10,000 m-thick Meso-Neoproterozoic succession (1.8–0.8 Ga) that records a complete rift cycle and is subdivided into four chronostratigraphic systems (Figure 3) (Wang et al. 2015; Liu, Zhang, et al. 2020; Meng et al. 2011). The basal Changcheng System (late Statherian) overlies Paleoproterozoic basement, comprising coastal to shallow-marine clastic deposits that mark the initial rift phase. The Changzhougou Formation (Chc) begins with poorly sorted, rounded, pebbly feldspathic coarse sandstone locally rich in quartzite clasts, transitioning upwards into purplish-grey, medium-thick bedded sandstone (Chen et al. 2014) (Figure 4). This unit exhibits large-scale trough and planar cross-bedding, wedge-shaped cross-bedding, wave ripples, and normal/inverse grading. Its relatively high quartz content, presence of feldspar and dark Fe-Mn detritus, and low textural maturity, combined with sedimentary structures like large cross-beds and ripples, indicate deposition in a high-energy beach/shoreface environment dominated by tidal processes during marine transgression, with paleocurrents suggesting provenance from the southwestern Wutai ancient land and Miyun-Huairou uplift (Chen et al. 2014). Overlying this, the Chuanlinggou Formation (Chch) consists predominantly of grey-black silty shale displaying fine laminations and horizontal bedding, with a distinctive tuffite marker bed in the middle (Liu et al. 2022) (Figure 4). The absence of coarse silt or sand, presence of pyrite nodules, and lack of bioturbation strongly suggest deposition in a low-energy, anoxic, reducing environment, interpreted as a restricted lagoon or bay, with local muddy tidal flats (Li, Ou, et al. 2020). The transitional Tuanshanzi Formation (Cht) exhibits a tripartite sequence: lower calcareous siltstone, middle haematite-bearing quartz sandstone, and upper stromatolite-bearing dolomite with chert bands. Characterized by interbedded sandstone, mudstone, and thin carbonate layers, along with wave ripples, lenticular bedding, and stromatolites, it represents a mixed tidal flat or restricted shallow marine setting, recording distinct transgressive-regressive cycles (Zhang et al. 2013). The Dahongyu Formation (Chd) provides critical evidence for syn-rift magmatism, characterized by interbedded K-rich trachyte, basalt, and tuffite volcanic flows and pyroclastics, which uncomfortably overlie the Tuanshanzi Formation (Xingcheng Movement) (Qu et al. 2012). Intercalated clastic sediments, primarily quartz sandstone and conglomerate (locally polymictic), deposited during volcanic quiescence, point to shallow marine or locally alluvial fan environments (Lu and Li 1991).

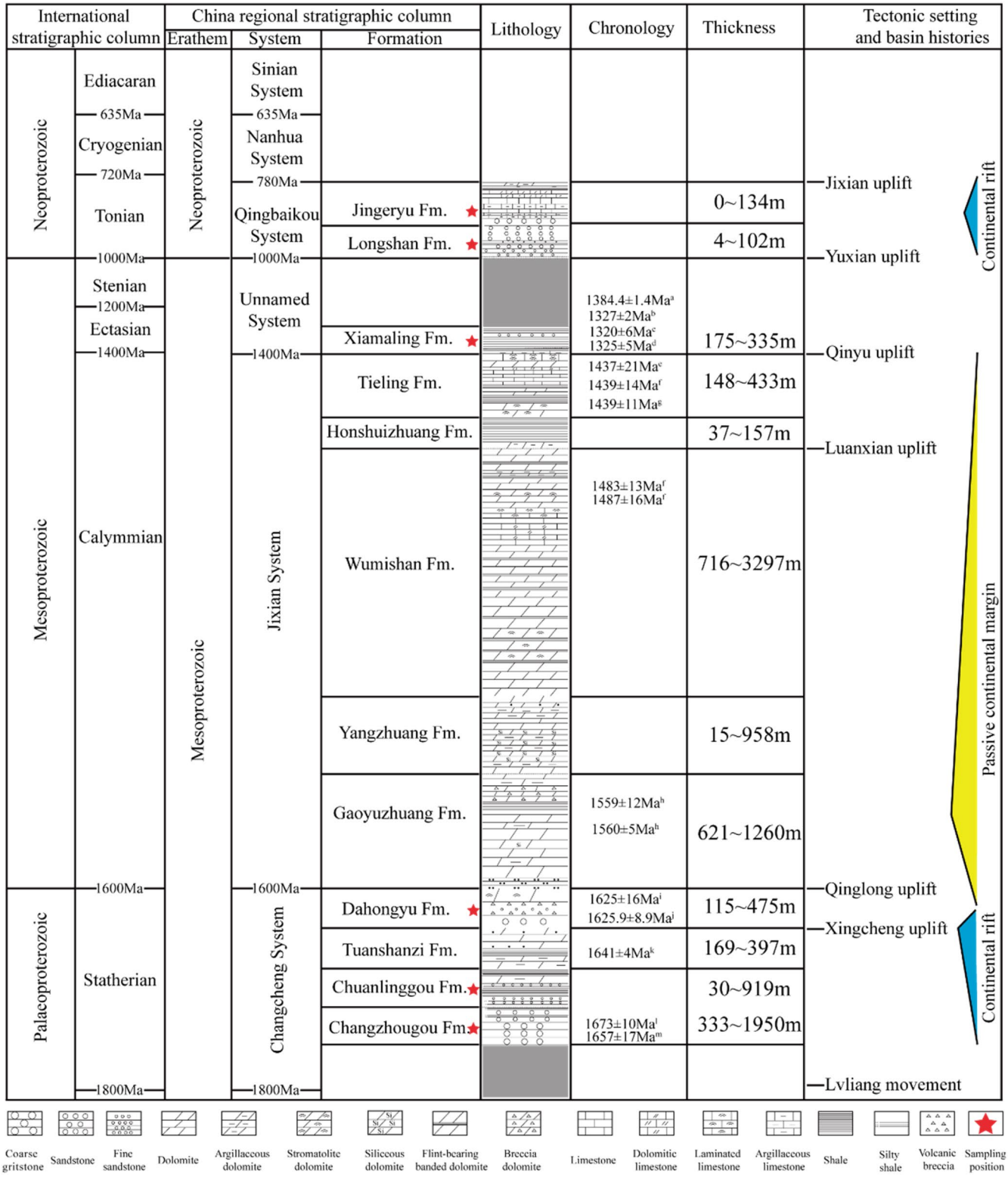

FIGURE 3 | Stratigraphic subdivision of the Meso-Neoproterozoic succession in Yan-Liao rift zone (modified after Zhai et al. 2015; Qu et al. 2010). Reference for chronology: (a) Zhang et al. (2015); (b) Liu et al. (2011); (c) Li et al. (2009); (d) Zhang et al. (2012); (e) Su et al. (2010); (f) Li et al. (2014); (g) Guo et al. (2019); (h) Li et al. (2010); (i) Lu et al. (2003); (j) Gao et al. (2008); (k) Zhang et al. (2013); (l) Li et al. (2011); (m) Duan et al. (2014).

Overlying the Changcheng System, the Jixian System (Calymmian) records a major shift to extensive carbonate platform deposition during the rift's main thermal subsidence phase, reflecting a period of stable tectonic setting and broad marine conditions (Gao and Zhu 2024). The Gaoyuzhuang Formation (Jxg) comprises thick-bedded, massive dolomite with chert bands and stromatolites; biomarker data showing high gammacerane and low Pr/Ph ratios indicate deposition in a hypersaline, reducing environment on a restricted to open carbonate platform (Sun et al. 2021). The Yangzhuang Formation

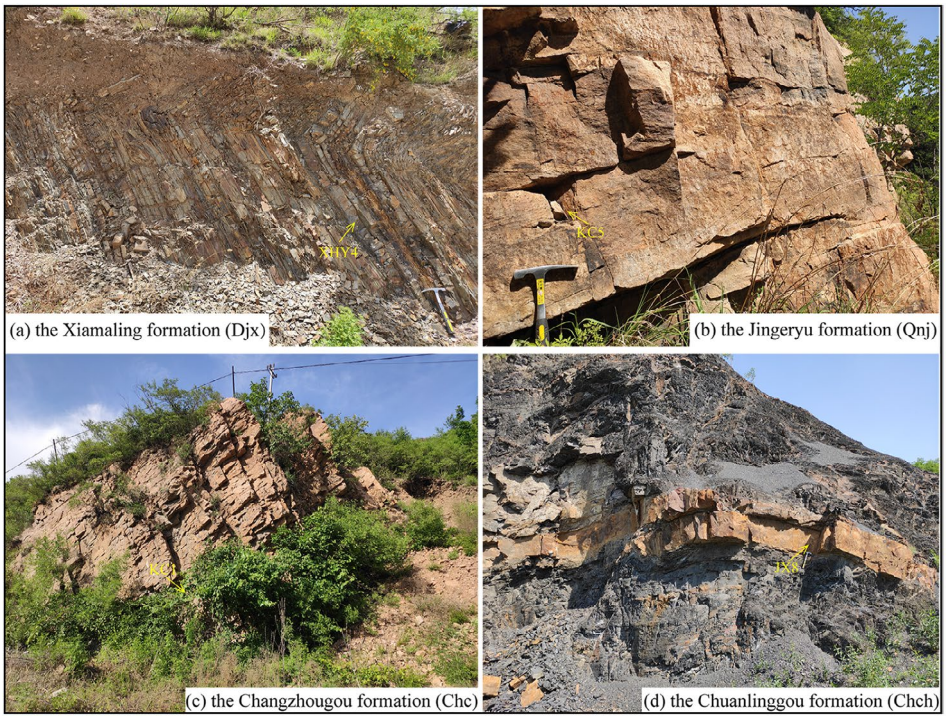

FIGURE 4 | Photographs of the field outcrops in the Yan-Liao rift zone. Image (a) shows the interbedding of mudstone and sandstone from the Xiamaling formation; Image (b) shows the quartz sandstone deposited in the Jingeryu formation; Image (c) shows the sandstone of the Changzhougou formation overlaying the metamorphic basement of the Paleoproterozoic era; Image (d) shows the sandstone bands embedded in shale of the Chuanlinggou formation.

(Jxy) features purple-red argillaceous dolomite containing gypsum pseudomorphs or nodules, clearly reflecting supratidal or restricted platform conditions under an arid climate (Qu et al. 2012). The exceptionally thick Wumishan Formation (Jxw) is dominated by thrombolitic and conical stromatolitic dolomite with abundant chert bands, representing a shallow subtidal to intertidal environment on a broad platform or ramp (Zheng 2016). The Hongshuizhuang Formation (Jxh) consists of black shale and mudstone rich in organic matter and pyrite, suggesting deposition in a deeper, anoxic intra-platform basin or outer shelf setting (Sun et al. 2021; Gao and Zhu 2024). The Tieling Formation (Jxt) is marked by stromatolitic limestone, capped by a prominent palaeokarst surface, indicating a final phase of open platform deposition followed by subaerial exposure (Gao and Zhu 2024).

A regionally significant unconformity (Qinyu Uplift) commonly separates the Tieling Formation from the overlying Unnamed System (Ectasian to Stenian), Xiamaling Formation (Djx). The Djx Formation shows a distinct sequence: basal sandstone, a thick main body of black shale (rich in organic matter and pyrite, locally containing graptolite fossils), and a capping sandstone (Gao, Zhang, Shi, Zhou, Wang, et al. 2007; Qiao et al. 2007) (Figure 4). The shales and the presence of glauconite in the sandstones indicate deposition in a deepening, oxygen-poor shelf environment, potentially related to a minor renewed subsidence pulse during cratonic adjustment (Qiao et al. 2007).

The terminal Qingbaikou System (Tonian) marks the rift demise phase (Li, Ou, et al. 2020). The Longshan Formation (Qnl) typically begins with a basal conglomerate or pebbly sandstone containing subangular to moderately rounded clasts of quartzite and granite, overlain by quartz arenites exhibiting large-scale cross-bedding. This unit shows evidence of tidal influence (bidirectional cross-bedding) and deposition within a tidal flat to shallow marine setting, rather than a braided fluvial environment. The upper part includes glauconite-bearing sandstones and purple-red shales (Guo et al. 2019). The Jingeryu Formation (Qnj) consists not only of purplish-red siltstones and mudstones but also includes basal sandstones and middle carbonate layers (dolomitic limestone) (Figure 4), indicating deposition in a mixed siliciclastic-carbonate tidal flat system under arid conditions (Song 2015). This succession signifies the cessation of significant Neoproterozoic sedimentation in the Yan-Liao rift zone. This sedimentary evolution—from initial rift-related coarse clastics (Chc, Chch) and volcanism (Chd) linked to active extension and basin formation, through a prolonged phase of widespread stable carbonate platform development (Jixian System) during thermal subsidence, punctuated by minor adjustments (Unnamed System), to final uplift and basin filling with mature sandstones and conglomerates (Qingbaikou System)—is diagnostic of an intracontinental rift basin (Zhai and Liu 2003; Peng et al. 2008; Wang et al. 2015).

Sampling targeted three areas within the central Yan-Liao rift zone (Figures 2 and 4) to capture stratigraphic and spatial variability (Guo et al. 2019; Sharman et al. 2018). In the Jixian area, hosting the thickest (~10,000 m), NNW-striking succession (Figure 2b), seven sandstone samples were collected from key formations representing different rift stages: Chc, Chch, Chd,

TABLE 1 | Samples information of the Yan-Liao rift zone.

Sample	Location	Lat.(N)	Lon.(E)	Formation	Rock type
XHY4	Xiahuayuan	40.46288	115.2325	Xiamaling (Dj*x*)	Quartzite
XHY6	Xiahuayuan	40.46879	115.26343	Xiamaling (Dj*x*)	Quartzite
KC1	Kuancheng	40.57241	118.55987	Changzhougou (Chc)	Quartz sandstone
KC2	Kuancheng	40.58327	118.54081	Chuanlinggou (Ch*ch*)	Quartz sandstone
KC4	Kuancheng	40.59107	118.52588	Dahongyu (Ch*d*)	Quartz sandstone
KC5	Kuancheng	40.61532	118.35838	Jingeryu (Qn*j*)	Quartz sandstone
JX1	Jixian	40.21807	117.51974	Changzhougou (Ch*c*)	Quartz sandstone
JX2	Jixian	40.20401	117.50675	Changzhougou (Ch*c*)	Quartz sandstone
JX3	Jixian	40.16861	117.48997	Dahongyu (Ch*d*)	Quartzite
JX8	Jixian	40.17588	117.50587	Chuanlinggou (Ch*ch*)	Quartz sandstone
JX10	Jixian	40.06689	117.43321	Jingeryu (Qn*j*)	Quartz sandstone
JX11	Jixian	40.07671	117.40497	Xiamaling (Dj*x*)	Quartzite
JX13	Jixian	40.07311	117.40962	Longshan (Qn*l*)	Feldspathic quartz sandstone

Djx, Qnl, and Qnj. Northeast of Jixian, the Kuancheng area exhibits NNE-striking strata with complete Meso-Neoproterozoic exposures except for the absent Djx Formation, yielding four samples from the Chc (shoreface sandstone), Chch, Chd, and Qnj units (Figure 4). To the west, the Xiahuayuan area provided two Djx Formation sandstones: XHY4 near Jurassic strata and XHY6 adjacent to the underlying Tieling Formation. Sample locations, lithostratigraphic affiliations, and GPS coordinates are detailed in Table 1.

3 | Analytical Methods

3.1 | LA-ICP-MS U–Pb Dating Method

Detrital zircon U–Pb geochronology was conducted at the Thermochronology Laboratory, China University of Petroleum (Beijing), utilising a New Wave 193 nm Excimer laser ablation (LA) system coupled to an Agilent 7900 inductively coupled plasma mass spectrometer (ICP-MS). Analytical protocols followed established methodologies to ensure data reproducibility and accuracy (Horstwood et al. 2016). NIST SRM 610 served as the external standard for elemental concentration calibration, with ^{91}Zr used as an internal standard to correct for instrumental drift (Chew et al. 2014). Age fractionation corrections were applied using the zircon reference material 91,500 (Wiedenbeck et al. 2004). To rigorously monitor analytical precision and accuracy throughout the analytical sessions, secondary zircon reference materials SA01 (Huang, Wang, et al. 2019; recommended age = 535.08 ± 0.32 Ma) and Plešovice (Sláma et al. 2008; recommended age = 337.13 ± 0.37 Ma) were analyzed intermittently alongside the unknowns. A total of 74 grains of SA01 yielded a concordia age of 536.37 ± 0.77 Ma (2σ; MSWD = 0.93), while 47 grains of Plešovice yielded a concordia age of 337.04 ± 0.63 Ma (2σ; MSWD = 2.2). Both results are concordant within 2% uncertainty of their respective recommended values (Spencer et al. 2016), validating the reliability of the analytical procedures and data reduction. Raw data were processed using the iolite v4 software package (Paton et al. 2011) with a customized data reduction scheme (DRS), with instrument operating parameters summarized in Table 2.

Given the polycyclic provenance of detrital zircons in Meso-Neoproterozoic strata, rigorous statistical validation of age spectra was prioritized. The probability of failure (P), quantifying the likelihood of incomplete sampling of age populations, was constrained to ≤ 5% (Dodson et al. 1988; Vermeesch 2004). As demonstrated by Vermeesch (2004), achieving this threshold requires a minimum of 117 concordant grains per sample. However, prolonged geological recycling in the Yan-Liao rift zone has likely perturbed U–Pb systematics, necessitating enhanced grain counts to mitigate partial resetting effects (Andersen et al. 2019). Consequently, between 160 and 320 zircon grains per sample were analyzed, selected based on cathodoluminescence zoning patterns and absence of visible inclusions or fractures (Figure 5). Detailed protocols for mineral separation, mounting, imaging, and data filtering are provided in the Supporting Informations.

3.2 | Maximum Depositional Age Calculation Methodology

Following U–Pb dating, we excluded individual grain ages with < 0.1 probability of concordance using IsoplotR (Vermeesch 2018). We implemented six complementary maximum depositional age (MDA) approaches: (1) the youngest graphical probability peak (YPP) (Dickinson and Gehrels 2009; Ludwig 2012); (2) the youngest single grain (YSG) age; (3–4) youngest grain clusters YGC1σ (grains overlapping at 1σ uncertainty) and YGC2σ (overlapping at 2σ uncertainty; Coutts et al. 2019); (5) the youngest statistical population (YSP; Coutts et al. 2019); and (6) the maximum likelihood age (MLA) (Vermeesch 2021). To accurately reveal sediment accumulation timing, we

TABLE 2 | Analytical parameters of LA-ICP-MS.

Laboratory and Sample Preparation	
Laboratory name	Thermochronology Laboratory, China University of Petroleum (Beijing)
Sample type	Detrital zircons
Sample preparation	Conventional mineral separation, 1 inch resin mount, 1 μm polish to finish
Laser Paremeters	
Instrument	New wave research 193 Ultra Compact
Laser wavelength	193 nm
Washout	15 s
Background	15 s
Ablation duration	45 s
Laster repetition rate	5 Hz
Sampling mode	Static spot ablation
Spot size	30 μm diameter spot
Energy	2.5 J/cm^2
Carrier gas1	900 mL/min He
Carrier gas2	3 m L/min N_2
Mass spectrometer parameters	
Instrument	Agilent 7900 ICP-MS
Sample introduction	Ablation aerosol
Detection system	Quadrupole mass analyzer
Forward power	1500 W
Reflect power	< 3 W
Dwell time	75 s
Plasma gas	Argon
Plasma gas flow	15 L/min
Carrier gas flow	0.7 L/min
Isotopes measured	^{91}Zr, ^{204}Pb, ^{206}Pb, ^{207}Pb, ^{208}Pb, ^{232}Th, ^{238}U

systematically compared these approaches across diverse depositional scenarios.

4 | Detrital Zircon U–Pb Results

4.1 | Detrital Zircon U–Pb Age Spectra

Detrital zircon U–Pb age distributions from Meso-Neoproterozoic strata in the Yan-Liao rift zone exhibit systematic variations. Samples from the Changzhougou Formation (Changcheng System; JX1, JX2, KC1) display strikingly similar age spectra, characterized by 92% of grains clustering between 2.7 and 2.2 Ga and a dominant peak at ~2.5 Ga (Figure 6). Moving to the overlying Chuanlinggou Formation, both JX8 (Jixian) and KC2 (Kuancheng) samples preserve the prominent ~2.5 Ga peak but also introduce secondary peaks within the 2.0–1.95 Ga range; nevertheless, 84% of grains still fall within the 2.7–2.2 Ga interval (Figure 6). A pronounced shift in provenance is evident in the Dahongyu Formation. Here, sample JX3 (Jixian) yielded exclusively Paleoproterozoic ages (1.9–1.5 Ga), whereas KC4 (Kuancheng) zircons retain Archean–Paleoproterozoic signatures (2.7–1.8 Ga) (Figure 6). Further complexity is recorded in the Xiamaling Formation, where JX11 (Jixian) and XHY6 (Xiahuayuan) share spectra dominated by 1.7–1.6 Ga ages, while the overlying sample XHY4 exhibits a broader range of older zircons (2.5–1.8 Ga) (Figure 6). Finally, within the terminal Qingbaikou System, the Longshan (JX13) and Jingeryu (JX10, KC5) formations show mixed Archean–Paleoproterozoic age populations but differ in their modal peaks (Figure 6). Cumulative distribution functions (CDFs) highlight four principal age clusters (1.6, 1.85, and 2.5 Ga) across the dataset (Figure 6).

4.2 | Detrital Zircon Morphological Parameters

Despite sharing statistically indistinguishable U–Pb age spectra, the Changzhougou Formation samples JX1, JX2, and KC1 exhibit systematic morphological trends. Specifically, mean grain size decreases progressively from JX1 to JX2 to KC1, with statistically significant differences observed. Concurrently, JX2 displays elevated aspect ratios and reduced circularity compared to both JX1 and KC1, although these differences in aspect ratio and circularity did not reach statistical significance (Figures 5 and 7). In contrast, Chuanlinggou Formation samples JX8 and KC2 exhibit statistically comparable grain sizes, aspect ratios, and circularity (Figures 5 and 7). Within the Dahongyu Formation, JX3 zircons are angular and poorly sorted, contrasting sharply with KC4 zircons, which exhibit high roundness (Figure 5). Similarly, in the Xiamaling Formation, JX11 and XHY6 zircons display angular to subangular morphologies, whereas XHY4 zircons are larger and rounded, with highly variable sorting (Figures 5 and 6). For the Qingbaikou System, JX13 (Longshan) zircons are moderately sorted and rounded, while JX10 and KC5 (Jingeryu) grains are smaller but similarly rounded; a progressive size reduction is noted from JX13 to JX10 to KC5 (Figure 6). Regarding zircon characteristics, Th/U ratios were greater than 0.4 for 87% of the 2442 grains analyzed (Figure 8), and cathodoluminescence (CL) images revealed zoning patterns including euhedral crystals and oscillatory zoning. However, 1% of grains exhibited anomalously low Th/U values (< 0.1).

5 | Discussion

5.1 | Detrital Zircon Ages and Their Implications for Estimating Maximum Depositional Ages

Applying the MDA estimation methodology outlined in Section 3.2 to our detrital zircon dataset reveals both the utility and limitations of these approaches within the evolving tectonic context of the Yan-Liao rift. For the Changzhougou Formation,

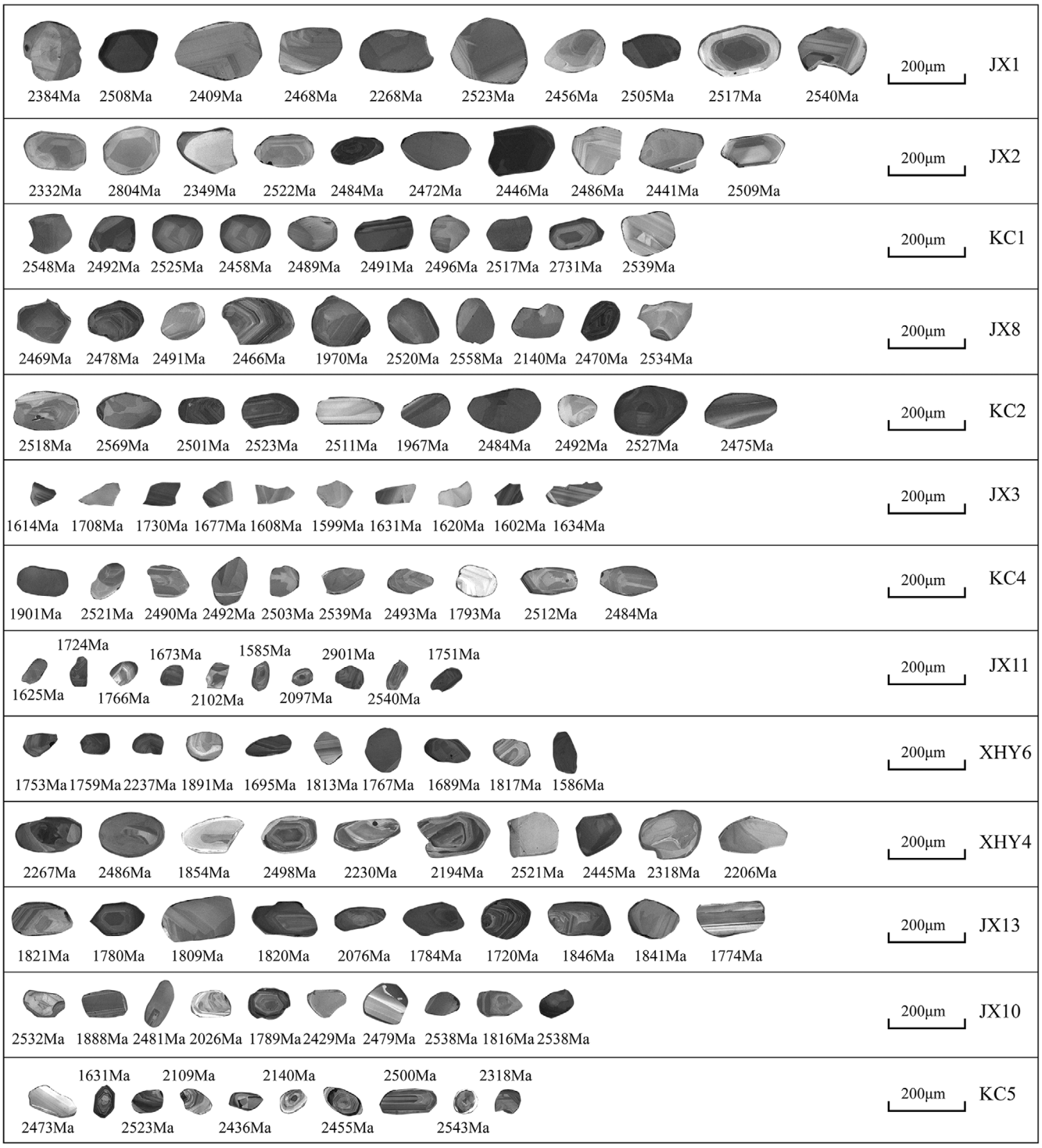

FIGURE 5 | Cathodoluminescence images of detrital zircons and their U–Pb ages. The photos of all grains were taken with the same scale, revealing significant differences in the morphology of zircon grains from older to younger strata.

the MLA age of 1653.3 Ma aligns well with recent volcanic interlayer dates (~1650 Ma; Li et al. 2013; Miao et al. 2019), validating the reliability of MLA in this relatively stable depositional setting. However, the anomalously older MDAs (> 1800 Ma) derived from cluster methods (Table 3), coupled with stratigraphic inversions observed in the overlying Chuanlinggou Formation MDA estimates, highlight significant methodological challenges. These occur when tectonic disruptions abruptly alter sediment sources, rendering the MLA ages ineffective for accurately constraining depositional timing. Volcaniclastic-rich units like the Dahongyu and Xiamaling formations exemplify proximity-driven biases. The short transport distances of syn-volcanic zircons (Figure 2) can cause YSG or MLA to underestimate the true MDA due to uncertainties in eruption duration and incorporation timing. In these cases, the YSP method yielded more robust estimates (1611.3 Ma and 1449.2 Ma, respectively), consistent with prior studies (Gao, Zhang, Shi, Zhou, Wang, et al. 2007; Zhang et al. 2015). Conversely, younger strata within

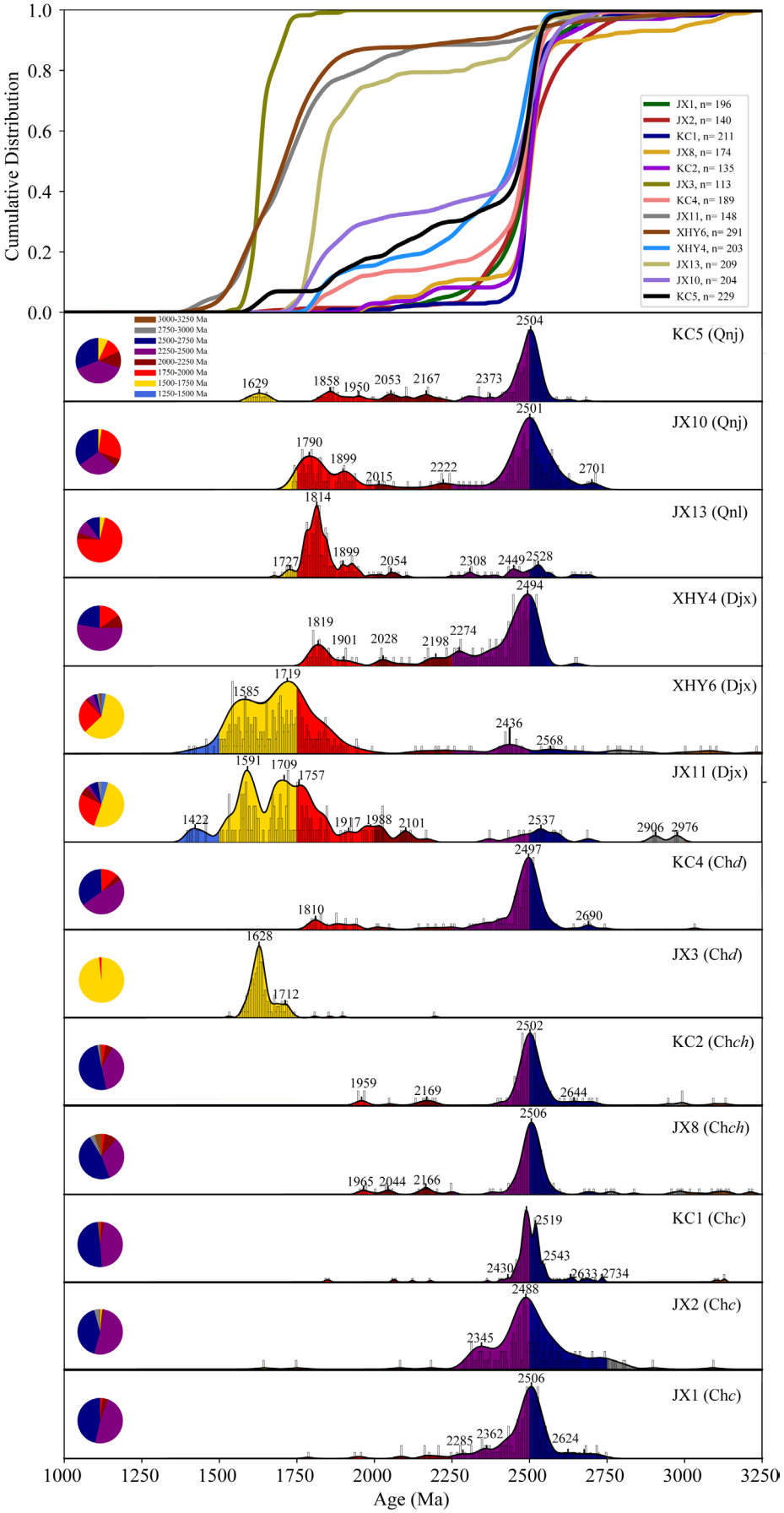

FIGURE 6 | Cumulative age distributions and kernel density estimates (KDE) of detrital zircons in the Yan-Liao rift zone: 250 Ma colour-coded intervals with grain proportion pie chart (right) and peak ages labelled (Ma).

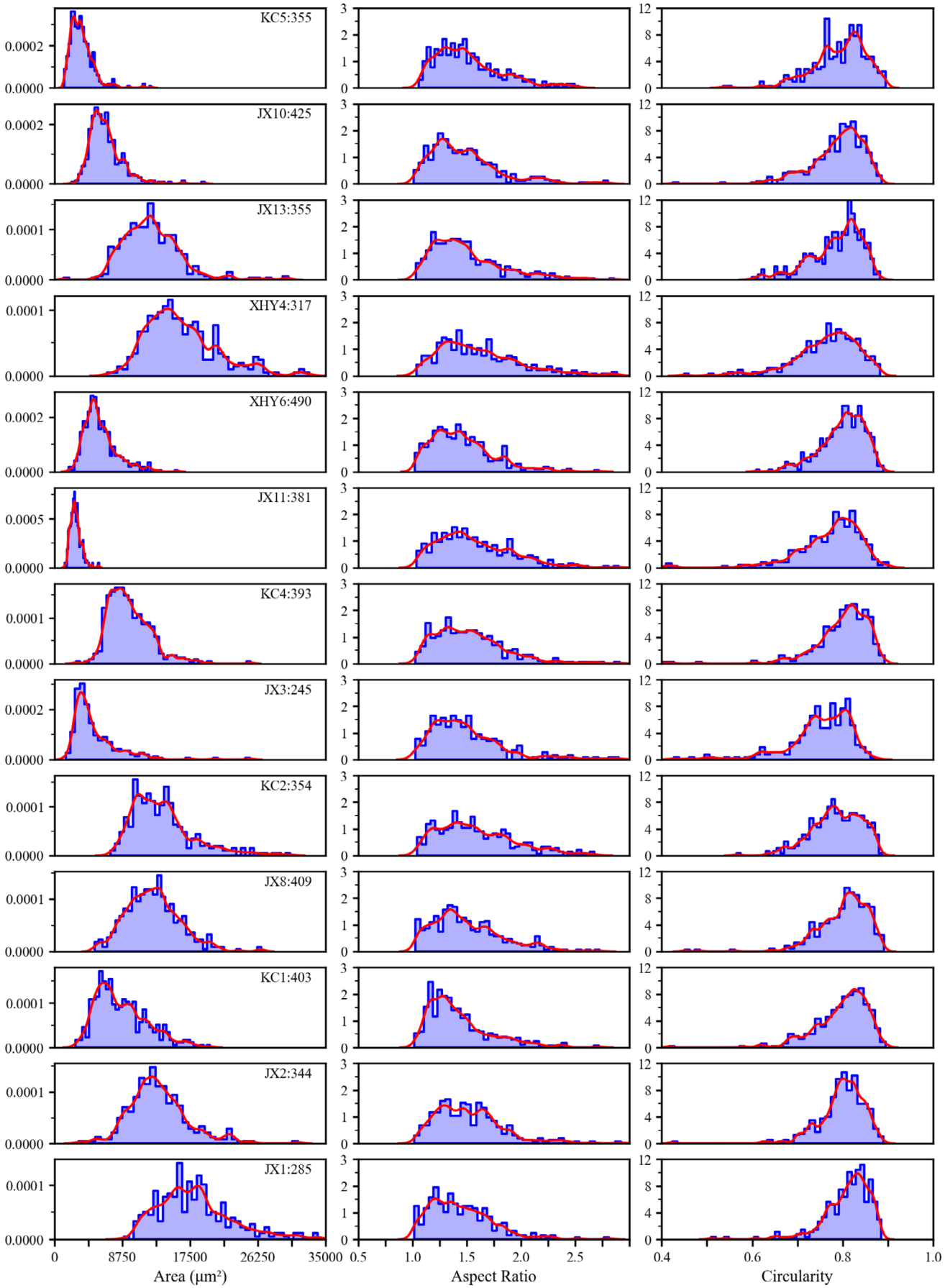

FIGURE 7 | Multiparametric particle morphology distributions across geological samples. The area, aspect ratio, and circularity comparative analysis via kernel density estimation.

the Qingbaikou System exhibit inherited age reversals similar to the Chuanlinggou Formation, underscoring the pervasive reorganization of source areas during late-stage rift evolution. These cases collectively emphasize the critical dependence of MDA fidelity on basin-to-source dynamics. While volcanic interlayers and biostratigraphy remain the most reliable chronostratigraphic tools where preserved (Sharman and Malkowski 2020), their scarcity in these rift basins necessitates the careful application and contextual interpretation of detrital zircon MDA methods, guided by integrated sedimentary facies analysis to identify potential recycled populations, especially where fault activity disrupts provenance signals.

5.2 | Provenance Analysis of Meso-Neoproterozoic Strata

Detrital zircon U–Pb age spectra (3.0–1.3 Ga) from the Yan-Liao rift zone's Meso-Neoproterozoic strata reveal a tectonic evolution marked by episodic magmatism and sediment confinement (Figure 6) (Cawood et al. 2012; Gehrels 2014). Histograms of zircon ages highlight dominant peaks at ~1.6, 1.85, 2.5, and 2.7 Ga (Figure 9). Cumulative distribution functions (CDFs) further delineate four principal age clusters (1.6, 1.85, 2.5, and 2.7 Ga; Figure 6), which correlate with major North China Craton (NCC) orogenic cycles: crustal growth (~2.9–2.7 Ga; Zhai et al. 2010), cratonization (~2.5 Ga; Santosh 2010), and Paleoproterozoic rifting (~1.8–1.6 Ga; Yang et al. 2005) (Figure 9). The origin of these zircons is supported by Th/U ratios and cathodoluminescence (CL) zoning patterns; specifically, Th/U ratios > 0.4 for 87% of grains and CL features like euhedral crystals and oscillatory zoning confirm dominantly magmatic origins for the majority of grains (Hoskin and Schaltegger 2003). However, anomalously low Th/U values (< 0.1) in 1% of grains likely reflect post-depositional metamorphic overprints or sedimentary recycling processes (Rubatto 2017), potentially linked to regional metamorphic events or reactivation of ancient basement of the North China Craton. The absence of 1.3–0.9 Ga zircons—a hallmark of the Xiong'er and Zhaertai-Bayan Obo-Huade rifts (Figure 1b)—reflects the Yan-Liao rift's unique provenance isolation, controlled by peripheral Archean uplifts and syn-rift magmatic architecture (Figure 11).

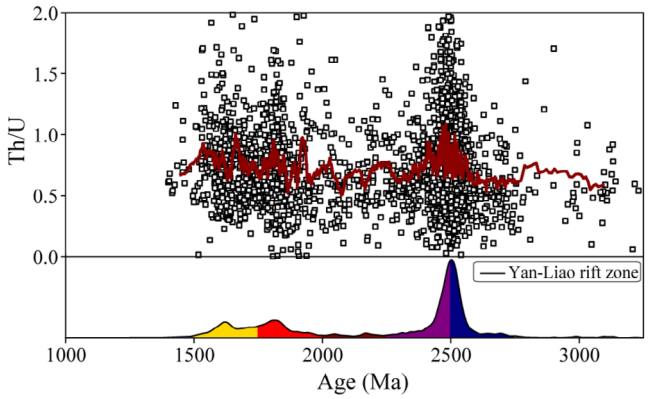

FIGURE 8 | Detrital zircon U–Pb ages and Th/U ratio distribution of Meso-Neoproterozoic samples.

Multidimensional scaling (MDS; Figure 10) delineates three distinct provenance regimes in the Yan-Liao rift zone, each corresponding to specific magmatic-tectonic phases. During the Statherian Changcheng System, the dominance of ~2.5 Ga zircons reflects recycling of Paleoproterozoic granites and metamorphic basement exposed along the rift margins (Figure 12), consistent with early rift-phase uplift and localized sediment derivation from ancient crustal blocks (Lu et al. 2017). In contrast, the Ectasian Dajian System records a pronounced shift to 1.8–1.4 Ga zircon populations, which align spatially and temporally with rift-axis magmatism (Figure 12). These younger zircons derive primarily from syn-sedimentary intrusions, including diorites (1.78–1.62 Ga; Ren et al. 2006) and syenogranites (1.68–1.55 Ga; Tapani Rämö et al. 1995), with proximal volcaniclastic inputs (Figure 11) minimizing sediment mixing and enhancing magmatic provenance signals. Subsequently, the Tonian Qingbaikou System exhibits a mixed zircon age spectrum combining ~2.5 Ga recycled basement components and 1.8–1.6 Ga intra-rift magmatic contributions (Figure 12). This dual sourcing reflects basement reactivation and spatially restricted sediment transport, as tectonic uplift partitioned the rift into isolated sub-basins with limited connectivity (Du and Tian 1985). The progressive transition from margin-dominated to rift-axis-centered provenances underscores the dynamic interplay between magmatic emplacement and basement exhumation.

5.3 | Paleogeographic Evolution of the Yan-Liao Rift Zone

The paleogeographic evolution of the Yan-Liao rift zone reflects dynamic interactions between tectonic regimes and sediment routing systems, as evidenced by provenance shifts, lithostratigraphic architecture, and unconformity patterns. During the late Statherian (~1.68 Ga), initial extension triggered rift basin development. Provenance data from the Changcheng System (dominant ~2.5 Ga zircons; Figure 6) indicate proximal sedimentation dominated by erosion of Archean-Paleoproterozoic (~2.5 Ga) basement uplifted along rift margins (Figure 12; Lu et al. 2017). This proximal sourcing is directly recorded by the lithology of the Changzhougou Formation (samples JX1, JX2, KC1), which comprises coarse-grained, poorly sorted conglomerates and feldspathic sandstones deposited in high-energy alluvial to braided fluvial systems. This is corroborated by detrital zircon morphological trends in the fluvial to shallow marine Changzhougou Formation (Figures 5 and 7): the statistically significant progressive decrease in mean grain size from JX1 to JX2 to KC1 aligns with increasing transport distance, indicating a transition from high-energy channel environments into lower-energy, shallow marine shoreline settings. This pattern is consistent with deposition in low-energy distal environments where prolonged sedimentary reworking enhanced hydraulic sorting and grain abrasion (Garzanti 2017), although the limited hydrodynamic energy resulted in abrasion dominated by mass loss rather than substantial geometric transformation (Sneed and Folk 1958), explaining the lack of significant differences in aspect ratio and circularity. Zircons from the overlying Chuanlinggou Formation (samples JX8, KC2) show statistically comparable grain sizes, aspect ratios, and circularity (Figures 5 and 7), reflecting persistently stable hydrodynamic conditions.

TABLE 3 | Maximum depositional age results of meso-neoproterozoic samples.

Sample	YSG (Ma)	YSG_2σ (Ma)	YGC1 (Ma)	YGC1_2σ (Ma)	YGC2 (Ma)	YGC2_2σ (Ma)	YPP (Ma)	YSP (Ma)	YSP_2σ (Ma)	MLA (Ma)	MLA_2σ (Ma)
JX1 (Ch*c*)	1785.3	48.8	1943.9	29.56	2184.8	17.2	1942.1	1943.9	29.57	1967.9	30.6
JX2 (Ch*c*)	1642.3	17.13	2294.6	13.88	2309.2	7.08	2315.9	2300.1	11.15	1653.3	19.7
KC1 (Ch*c*)	1843.9	34.3	1849.4	23.28	2091.9	7.08	1536.7	1849.4	23.28	1905.9	26.29
JX8 (Ch*ch*)	1951.1	27.35	1964.9	11.68	1972.6	19.14	1966.5	1963	13.35	1968.6	14.69
KC2 (Ch*ch*)	1947	27.71	1961	10.48	1961	10.48	1792.9	1961	10.49	1957.9	15.29
JX3 (Ch*d*)	1530.1	23.8	1590.6	7.6	1608.1	4.4	1440.5	1611.3	3.4	1584.3	8.367
KC4 (Ch*d*)	1783	31.84	1800.1	10.88	1812.3	7.22	1812.8	1807.9	8.2	1810.9	16.59
JX11 (Dj*x*)	1399.5	37.17	1415.3	19.2	1431.4	14.88	1849.5	1425.2	16.42	1431.1	26.76
XHY6 (Dj*x*)	1403	61.59	1437.8	26.98	1449.2	23.04	1964.9	1449.2	23.05	1481.8	17.12
XHY4 (Dj*x*)	1784.9	18.28	1794.7	8.66	1797.8	7.66	1811.1	1802.7	6.6	1784.9	14.7
JX13 (Qn*l*)	999.5	50.68	1731.9	18.04	1766.9	7.98	1625.1	1767.3	7.03	1636.7	83.87
JX10 (Qn*j*)	1736	87.52	1773.8	13.62	1792.4	11.06	1804.3	1799.5	10.5	1787.9	17.31
KC5 (Qn*j*)	1590.2	26.5	1601.3	11.8	1615.9	8.06	1580.7	1609	9.47	1605.4	19.18

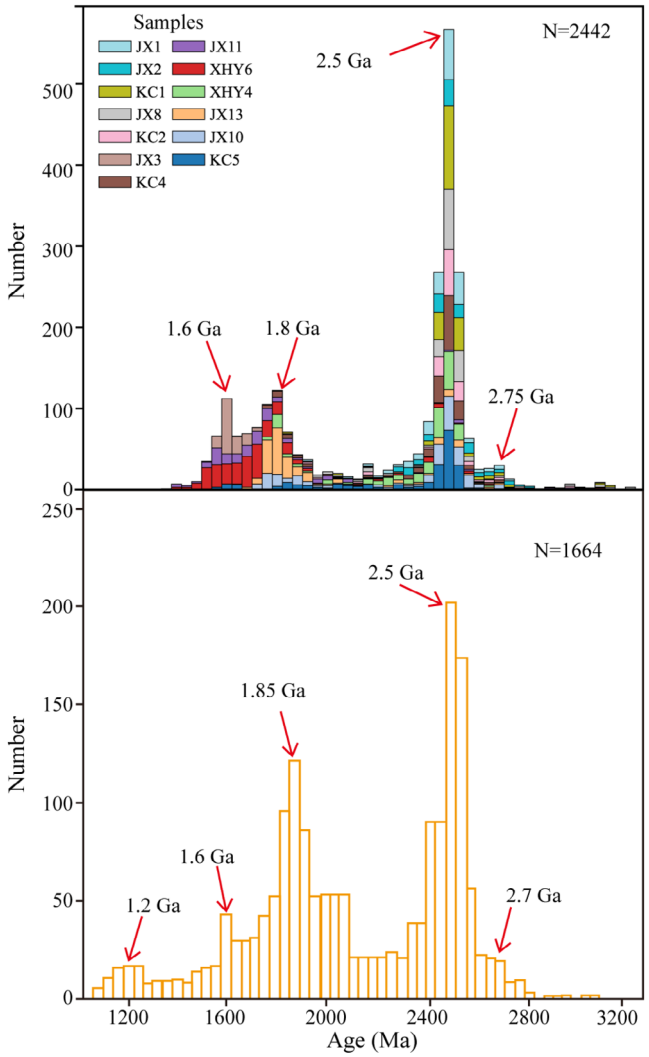

FIGURE 9 | Aggregated detrital zircon age histograms (40 Ma bin width) combining data from the Yan-Liao rift zone (this study) and the North China Craton (after Zhai et al. 2014).

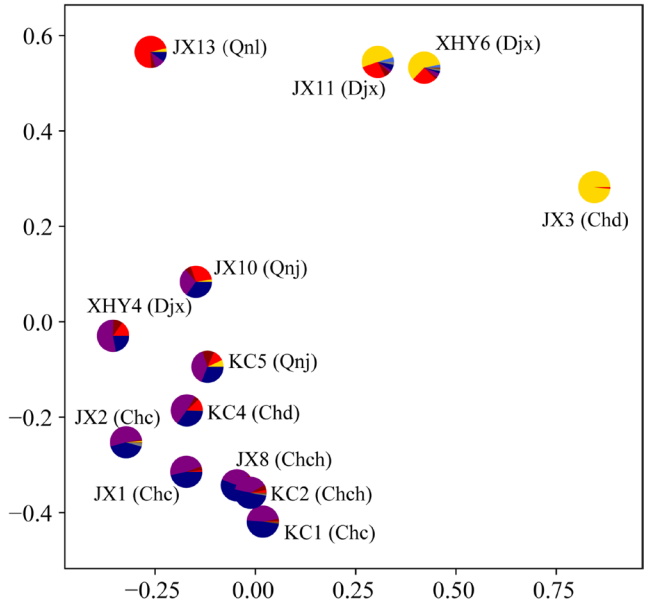

FIGURE 10 | Multi-dimensional scaling (MDS) plots, with pie chart colours referencing the age ranges defined in Figure 6. Inter-point distances reflect dissimilarity in age distributions between samples.

Synchronous volcanic activity in the central Jixian area introduced localized 1.62 Ga zircons in the Dahongyu Formation (sample JX3), while peripheral Kuancheng regions remained reliant on ancient uplift erosion, as evidenced by the rounded zircon morphology of Dahongyu Formation sample KC4 contrasting with JX3's angular grains (Figure 5).

Transition to the Calymmian (1.6–1.4 Ga) was marked by a major marine transgression, leading to deepened water conditions and the development of an extensive shallow marine environment (Pan et al. 2013). This facilitated widespread carbonate platform deposition (Jixian System), with uniform lithology and thickness reflecting stable thermal subsidence (Figure 12).

Renewed extension during the Ectasian (1.4–1.2 Ga) is marked by sedimentation of the Unnamed System. Organic-rich black shales of the Xiamaling Formation (samples XHY6, JX11) were deposited in deep-water anoxic basins—potentially linked to global Large Igneous Province events (Zhang et al. 2022). Similar 1.7–1.6 Ga zircon populations in XHY6 and JX11 (Figure 8) suggest intra-rift magmatic sourcing, coinciding with active margin subduction along the northern NCC (Qu et al. 2010). The angular to subangular morphologies of zircons in these samples (Figures 5 and 6) signal relatively rapid erosion and short-distance transport from these newly active magmatic sources. In contrast, the overlying Xiamaling Formation sample XHY4 exhibits larger, rounded zircons with older ages (2.5–1.8 Ga) and highly variable sorting (Figures 5 and 6), suggesting a pronounced shift to a distal, lower-energy depositional setting involving reworking of older basement material (Spencer et al. 2018).

Neoproterozoic Tonian uplift (Qingbaikou System, 1.2–0.9 Ga) reorganized sediment dynamics and caused regional shallowing. Mixed ~2.5 Ga and 1.8–1.6 Ga zircons in the Longshan Formation (samples JX13, JX10) and Jingeryu Formation (sample KC5) (Figure 6) record both basement re-exhumation and localized magmatism (Figure 12). Detrital zircon morphology shows JX13 (Longshan Formation) zircons are moderately sorted and rounded, while JX10 (Longshan Formation) and KC5 (Jingeryu Formation) grains are smaller but similarly rounded; a progressive size reduction is noted from JX13 to JX10 to KC5 (Figure 6). Despite comparable roundness, this progressive size reduction implies waning sediment flux energy during late rift evolution. The depositional environment evolved from nearshore (Longshan Formation) to a tidally influenced shallow marine carbonate platform (Jingeryu Formation), forming a classic transgressive succession from shoreline sandstones to laminated limestones (Li, Wei, et al. 2020). The absence of 1.3–0.9 Ga zircons—ubiquitous in adjacent NCC rifts—confirms the Yan-Liao basin's isolation by sustained peripheral uplifts, restricting Grenvillian-age inputs (Figure 12). This closure contrasts with the Xiong'er and Zhaertai-Bayan Obo-Huade rifts, where broader sediment mixing persisted.

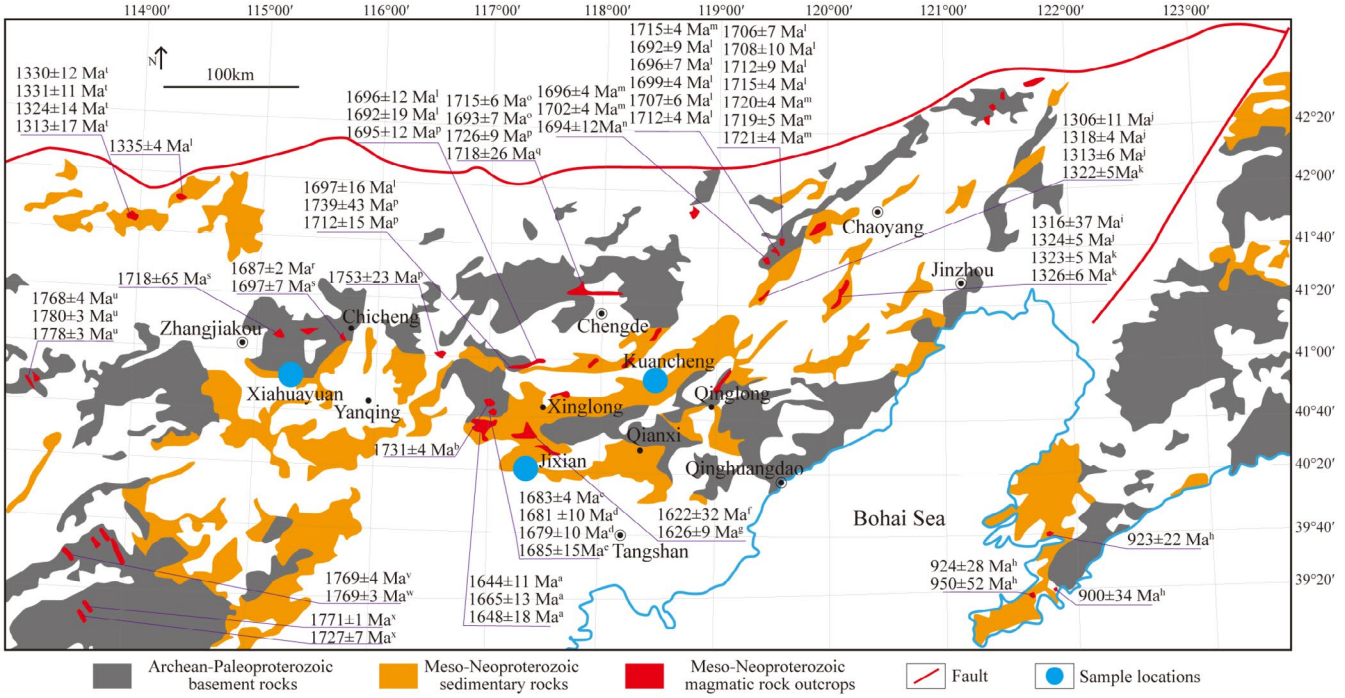

FIGURE 11 | Distribution and age of Meso-Neoproterozoic strata and magmatic rocks in the northern margin of the North China Craton. Reference for chronology: (a) Wang et al. (2015); (b) Peng et al. (2012); (c) Tapani Rämö et al. (1995); (d) Yang et al. (2005); (e) Gao et al. (2008); (f) Lu et al. (2008); (g) Gao et al. (2008); (h) Zhang et al. (2016); (i) Zhang et al. (2012); (j) Zhang et al. (2017); (k) Wang et al. (2014); (l) Hu et al. (2012); (m) Wang et al. (2013); (n) Liu et al. (2011); (o) Zhao et al. (2004); (p) Zhang, Zhang, et al. (2007); (q) Ren et al. (2006); (r) Zhang, Liu, et al. (2007); (s) Mo et al. (1997); (t) Zhang et al. (2012); (u) Wang et al. (2016); (v) Han et al. (2007); (w) Li et al. (2001); (x) Peng (2015).

5.4 | Geological Insights Into the Supercontinent Cycle Through Continental Rift Evolution

The Yan-Liao rift zone preserves a critical record of continental rifting and supercontinent interaction, as demonstrated by our new detrital zircon U–Pb datasets (1.8–1.4 Ga) and stratigraphic correlations. During the Statherian to Calymmian (1.8–1.6 Ga), peak magmatic activity—evidenced by dominant zircon age components at 1.8–1.6 Ga (Figure 12)—coincides with the terminal breakup of the Columbia supercontinent, consistent with global patterns of lithospheric extension and mantle upwelling (Zhai and Santosh 2013). This phase is marked by widespread volcaniclastic sedimentation and rift-related anorogenic magmatism, mirroring coeval rift systems in Laurentia and Baltica (Li et al. 2019; Pourteau et al. 2018).

The transition to passive margin sedimentation (~1600–1400 Ma) is characterized by carbonate-dominated sequences and a pronounced decline in juvenile zircon contributions (Figure 12), reflecting tectonic stabilization and enhanced sediment recycling from cratonic interiors. This shift parallels the NCC's integration into a broader passive margin regime, as inferred from regional stratigraphic correlations (Hofmann and Chen 1981; Tan et al. 2021). However, the absence of 1.3–1.0 Ga zircons in the Yan-Liao rift contrasts sharply with their preservation in the western Zhaertai rift and eastern Jiaoliao region (Zhang et al. 2021), suggesting differential uplift during Rodinia assembly. This hiatus, correlative with Grenvillian orogenesis (Liu, Zhao, et al. 2020), implies compressive stresses propagated into the NCC's interior, despite limited direct magmatic evidence—a pattern consistent with peripheral foreland basin dynamics during supercontinent amalgamation (Huang, Yuan, et al. 2019).

Spatial heterogeneity in Ectasian sediment provenance further underscores tectonic reorganization. While early Ectasian samples (JX13, XHY4) exhibit uniform age distributions indicative of stable cratonic sourcing, later stages (e.g., XHY6) show provenance shifts toward reactivated ancient uplifts (Dong et al. 2012). This trend, coupled with westward migration of the sedimentary depocenter (Guo et al. 2019), highlights intensified marginal tectonic activity during Rodinia's assembly. Crucially, the limited influx of distal sediments—contrasted by Fennoscandian-derived Mesoproterozoic zircons in the Langshan-Zha'ertai-Bayan Obo-Huade rift (Liu, Zhang, et al. 2020)—emphasizes the Yan-Liao rift's isolation under persistent flanking uplifts (Pan et al. 2013). These findings reconcile previous discrepancies: the Yan-Liao rift's episodic rifting and uplift reflect dual supercontinent cycles, with Columbia's fragmentation driving early extension and Rodinia's assembly inducing compression. The scarcity of 1300–1000 Ma zircons does not negate NCC's involvement in Rodinia but rather signals erosional stripping during uplift, as evidenced by fragmented Xiamaling Formation remnants (Qu et al. 2010).

6 | Conclusions

This integrated study of Meso-Neoproterozoic clastic successions in the Yan-Liao rift zone, North China Craton (NCC), combines

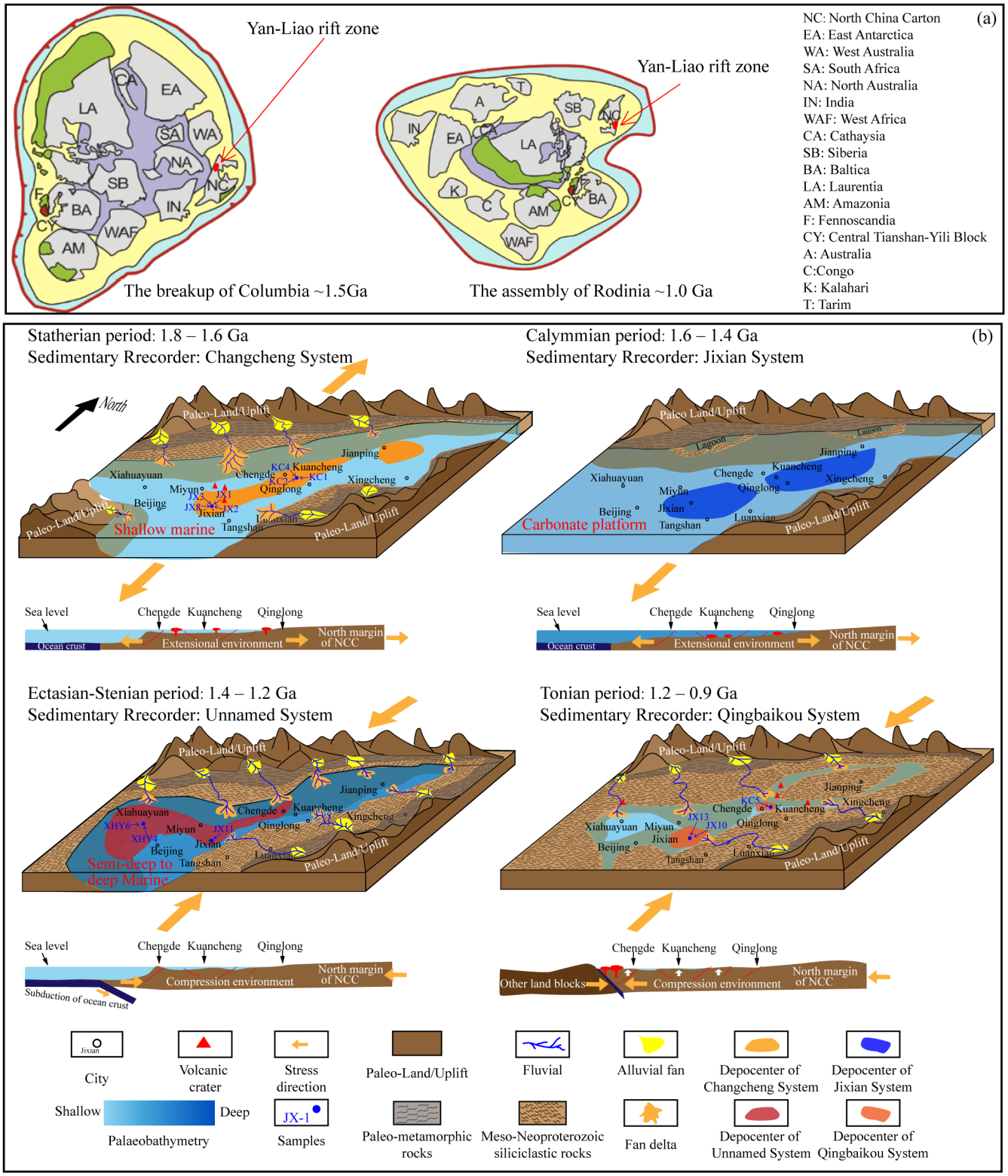

FIGURE 12 | (a) Paleogeographic reconstruction showing the locations of continental blocks during the breakup of Columbia and the assembly of Rodinia, with the position of the Yan-Liao rift zone within the North China Craton; (b) Integrated tectonic-sedimentary evolution model of the Yan-Liao rift zone along the northern margin of the North China Craton during the Meso-Neoproterozoic (1.8–1.0 Ga), illustrating the influence of supercontinent cycles: Extension (1.8–1.4 Ga), compression (1.4–1.0 Ga), sea-level fluctuations, migration of depocenters, and major provenance areas (paleo-uplifts, ancient metamorphic rocks, and overlying Paleoproterozoic strata). (Modified after Li, Wei, et al. 2020; Meng et al. 2011; Liu, Zhang, et al. 2020; Huang, Yuan, et al. 2019).

detrital zircon U–Pb geochronology ($n = 2442$), stratigraphic analysis, and paleogeographic reconstructions to elucidate tectonic and sedimentary responses to supercontinent cycles. The detrital zircon record reveals four dominant age peaks (2.75, 2.5, 1.85, and 1.6 Ga), with pre-1.8 Ga populations sourced from reworked Archean to Paleoproterozoic basement, while younger zircons (1.8–1.4 Ga) reflect syn-rift Mesoproterozoic magmatism. Provenance contrasts between distal and proximal settings demonstrate that maximum depositional ages (MDAs) are best constrained by the MLA ages in distal deposits but require the YSP ages in proximal volcaniclastic units, where rapid sedimentation and localized magmatism distort statistical population interpretations. Four distinct paleogeographic stages—initial rifting (1.8–1.6 Ga), passive margin development (1.6–1.4 Ga), intracontinental subsidence (1.4–1.2 Ga), and Tonian uplift (1.0–0.9 Ga)—highlight the rift's dynamic evolution from Columbia breakup to Rodinia assembly. The absence of 1.3–0.9 Ga zircons, ubiquitous in adjacent NCC rift systems, underscores the Yan-Liao basin's isolation by sustained peripheral uplifts during Rodinia amalgamation, which restricted sediment influx and preserved a fragmented stratigraphic record. These findings position the Yan-Liao rift as a critical archive of NCC's dual supercontinent interactions: Columbia's fragmentation drove early extensional magmatism and rift-basin formation, while Rodinia's assembly induced compressional uplift and provenance reorganization, erasing Grenvillian-age sedimentary records.

Acknowledgements

This study was supported by the National Key R&D Program of China (Grant No. 2017YFC0603102).

Conflicts of Interest

The authors declare no conflicts of interest.

Data Availability Statement

The data that supports the findings of this study are available in the Supporting Information of this article.

References

Andersen, T., M. A. Elburg, and B. N. Magwaza. 2019. "Sources of Bias in Detrital Zircon Geochronology: Discordance, Concealed Lead Loss and Common Lead Correction." *Earth-Science Reviews* 197: 102899.

Caracciolo, L. 2020. "Sediment Generation and Sediment Routing Systems From a Quantitative Provenance Analysis Perspective: Review, Application and Future Development." *Earth-Science Reviews* 209: 103226.

Cawood, P. A., C. J. Hawkesworth, and B. Dhuime. 2012. "Detrital Zircon Record and Tectonic Setting." *Geology* 40: 875–878.

Chen, X., C. Zhang, J. Liu, and O. Tegusi. 2014. "Fluvial Facies in the Changzhougou Formation in the Jixian Area of China and Geological Significance." *Journal of Stratigraphy* 38: 236–244.

Chew, D. M., J. A. Petrus, and B. S. Kamber. 2014. "U–pb LA–ICPMS Dating Using Accessory Mineral Standards With Variable Common pb." *Chemical Geology* 363: 185–199.

Coutts, D. S., W. A. Matthews, and S. M. Hubbard. 2019. "Assessment of Widely Used Methods to Derive Depositional Ages From Detrital Zircon Populations." *Geoscience Frontiers* 10: 1421–1435.

Deng, Y., H. Wang, D. Lyu, et al. 2021. "Evolution of the 1.8–1.6 Ga Yanliao and Xiong'er Basins, North China Craton." *Precambrian Research* 365: 106383.

Dickinson, W. R., and G. E. Gehrels. 2009. "Use of U–pb Ages of Detrital Zircons to Infer Maximum Depositional Ages of Strata: A Test Against a Colorado Plateau Mesozoic Database." *Earth and Planetary Science Letters* 288, no. 1–2: 115–125.

Dickinson, W. R., M. A. Klute, M. J. Hayes, et al. 1988. "Paleogeographic and Paleotectonic Setting of Laramide Sedimentary Basins in the Central Rocky Mountain Region." *Geological Society of America Bulletin* 100: 1023–1039.

Dodson, M. H., W. Compston, I. S. Williams, and J. F. Wilson. 1988. "A Search for Ancient Detrital Zircons in Zimbabwean Sediments." *Journal of the Geological Society* 145: 977–983.

Dong, Z., Z. Meisheng, and W. Yini. 2012. "Strati-Graphic Sequence and Sedimentary Environment of the Haifang-Gou Formation in the Longhuitou Basin of Xingcheng, Liaoning Province." *Geology and Exploration* 48: 227–236.

Du, R., and L. Tian. 1985. "Algal Macrofossils From the Qingbaikou System in the Yanshan Range of North China." *Precambrian Research* 29: 5–14.

Duan, C., Y. Li, M. Wei, et al. 2014. "U-Pb Dating Study of Detrital Zircons from the Chuanlinggou Formation in Jiangjiazhai Iron Deposit, North China Craton and Its Geological Significances." *Acta Petrologica Sinica* 30: 35–48.

Fonneland, H. C., T. Lien, O. J. Martinsen, R. B. Pedersen, and J. Košler. 2004. "Detrital Zircon Ages: A Key to Understanding the Deposition of Deep Marine Sandstones in the Norwegian Sea." *Sedimentary Geology* 164: 147–159.

Gao, L., C. Zhang, X. Shi, B. Song, Z. Wang, and Y. Liu. 2008. "Mesoproterozoic Age for Xiamaling Formation in North China Plate Indicated by Zircon SHRIMP Dating." *Chinese Science Bulletin* 53: 2665–2671.

Gao, L., C. Zhang, X. Shi, H. Zhou, Z. Wang, and B. Song. 2007. "A New SHRIMP Age of the Xiamaling Formation in the North China Plate and Its Geological Significance." *Acta Geologica Sinica-English Edition* 81: 1103–1109.

Gao, Z. F., and X. K. Zhu. 2024. "Sulfur Isotopic Characteristics of the Gaobanhe Deposit in East Hebei Province and Their Constraints on the Processes of Sulfide and Mn Mineralization From the Gaoyuzhuang Formation." *Acta Petrologica Sinica* 40: 267–281.

Garzanti, E. 2017. "The Maturity Myth in Sedimentology and Provenance Analysis." *Journal of Sedimentary Research* 87: 353–365.

Garzanti, E., and S. Andò. 2007. "Heavy Mineral Concentration in Modern Sands: Implications for Provenance Interpretation." *Developments in Sedimentology* 58: 517–545.

Garzanti, E., P. Vermeesch, M. Padoan, A. Resentini, G. Vezzoli, and S. Andò. 2014. "Provenance of Passive-Margin Sand (Southern Africa)." *Journal of Geology* 122: 17–42. https://doi.org/10.1086/674803.

Gehrels, G. 2014. "Detrital Zircon U-Pb Geochronology Applied to Tectonics." *Annual Review of Earth and Planetary Sciences* 42: 127–149.

Geisler, T., A. A. Rashwan, M. K. W. Rahn, et al. 2003. "Low-Temperature Hydrothermal Alteration of Natural Metamict Zircons From the Eastern Desert, Egypt." *Mineralogical Magazine* 67: 485–508.

Guo, Q., Z. Jin, X. Zhu, et al. 2019. "Sedimentar y Facies Evolution of the Neoproterozoic in Qingbaikou Area of Jingxi Depression, Yanshan Region." *Journal of Palaeogeography (Chinese Edition)* 21: 422–430.

Han, B., L. Zhang, Y. Wang, and B. Song. 2007. "Enriched Mantle Source for Paleoproterozoic High Mg and Low Ti-P Mafic Dykes in Central Part of the North China Craton: Constraints from Zircon Hf Isotopic Compositions." *Acta Petrologica Sinica* 23: 277–284.

He, Z., X. Meng, and M. Ge. 1994. "Environmental Evolutions and Structural Control of Changchengian of the Mid-Proterozoic in the Yanshan Basin, North China." *Acta Sedimentologica Sinica* 12: 10–19.

Herriott, T. M., J. L. Crowley, M. D. Schmitz, M. A. Wartes, and R. J. Gillis. 2019. "Exploring the Law of Detrital Zircon: LA-ICP-MS and CA-TIMS Geochronology of Jurassic Forearc Strata, Cook Inlet, Alaska, USA." *Geology* 47: 1044–1048.

Hofmann, H., and J. Chen. 1981. "Carbonaceous Megafossils From the Precambrian (1800 Ma) Near Jixian, Northern China." *Canadian Journal of Earth Sciences* 18: 443–447.

Horstwood, M. S. A., J. Košler, G. Gehrels, et al. 2016. "Community-Derived Standards for La-Icp-Ms U-(Th-)Pb Geochronology – Uncertainty Propagation, Age Interpretation and Data Reporting." *Geostandards and Geoanalytical Research* 40: 311–332.

Horton, B. K., V. J. Anderson, V. Caballero, et al. 2015. "Application of Detrital Zircon U-Pb Geochronology to Surface and Subsurface Correlations of Provenance, Paleodrainage, and Tectonics of the Middle Magdalena Valley Basin of Colombia." *Geosphere* 11: 1790–1811.

Hoskin, P. W. O., and U. Schaltegger. 2003. "The Composition of Zircon and Igneous and Metamorphic Petrogenesis." *Reviews in Mineralogy and Geochemistry* 53: 27–62.

Hou, G., J. Li, M. Yang, W. Yao, C. Wang, and Y. Wang. 2008. "Geochemical Constraints on the Tectonic Environment of the Late Paleoproterozoic Mafic Dyke Swarms in the North China Craton." *Gondwana Research* 13: 103–116.

Hu, B., M. Zhai, T. Li, et al. 2012. "Mesoproterozoic Magmatic Events in the Eastern North China Craton and Their Tectonic Implications: Geochronological Evidence from Detrital Zircons in the Shandong Peninsula and North Korea." *Gondwana Research* 22: 828–842.

Huang, C., H. Wang, J. Yang, et al. 2019. "SA01 – A Proposed Zircon Reference Material for Microbeam U-Pb Age and hf-O Isotopic Determination." *Geostandards and Geoanalytical Research* 44: 103–123.

Huang, Z., C. Yuan, X. Long, Y. Zhang, and L. Du. 2019. "From Breakup of Nuna to Assembly of Rodinia: A Link Between the Chinese Central Tianshan Block and Fennoscandia." *Tectonics* 38: 4378–4398.

Johnsson, M. J. 1993. "The System Controlling the Composition of Clastic Sediments." In *Processes Controlling the Composition of Clastic Sediments*. Edited by M. J. Johnsson, and A. Basu, Geological Society of America. https://doi.org/10.1130/SPE284-p1.

Kennedy, A., M. Lagos, and C. Ballhaus. 2003. "Zircons From Syros, Cyclades, Greece – Recrystallization and Mobilization of Zircon During High-Pressure Metamorphism." *Journal of Petrology* 44: 1977–2002.

Kuang, H., Y. Liu, Y. Geng, et al. 2019. "Important Sedimentary Geological Events of the Meso-Neoproterozoic and Their Significance." *Journal of Palaeogeography (Chinese Edition)* 21: 1–30.

Kusky, T., B. Windley, and G. Zhai. 2007. "Tectonic Evolution of the North China Block: From Orogen to Craton to Orogen." *Geological Society, London, Special Publications* 280: 1–34.

Li, H., S. Lu, H. Li, et al. 2009. "Zircon and Beddeleyite U-Pb Precision Dating of Basic Rock Sills Intruding Xiamaling Formation, North China." *Geological Bulletin of China* 28: 1396–1404.

Li, H., S. Lu, W. Su, Z. Xiang, H. Zhou, and Y. Zhang. 2013. "Recent Advances in the Study of the Mesoproterozoic Geochronology in the North China Craton." *Journal of Asian Earth Sciences* 72: 216–227.

Li, H., W. Su, H. Zhou, et al. 2011. "The Base Age of the Changchengian System at the Northern North China Craton Should Be Younger Than 1670 Ma: Constraints From Zircon U-Pb LA-MC-ICPMS Dating of a Granite-Porphyry Dike in Miyun County, Beijing." *Earth Science Frontiers* 18: 108–120.

Li, H., W. Su, H. Zhou, et al. 2014. "The First Precise Age Constraints on the Jixian System of the Meso-to Neoproterozoic Standard Section of China: Shrimp Zircon U-Pb Dating of Bentonites from the Wumishan and Tieling Formations in the Jixian Section, North China Craton." *Acta Petrologica Sinica* 30: 2999–3012.

Li, H., S. Zhu, Z. Xiang, et al. 2010. "Zircon U-Pb Dating on Tuff Bed from Gaoyuzhuang Formation in Yanqing, Beijing: Further Constraints on the New Subdivision of the Mesoproterozoic Stratigraphy in the Northern North China Craton." *Acta Petrologica Sinica* 26: 2131–2140.

Li, J., G. Hou, X. Qian, H. C. Halls, and D. Davis. 2001. "Single-Zircon U-Pb Age of the Initial Mesoproterozoic Basic Dike Swarms in Hengshan Mountain and Its Implication for the Tectonic Evolution of the North China Craton." *Geological Review* 47: 234–238.

Li, S., X. Li, G. Wang, et al. 2019. "Global Meso-Neoproterozoic Plate Reconstruction and Formation Mechanism for Precambrian Basins: Constraints From Three Cratons in China." *Earth-Science Reviews* 198: 102946.

Li, X., Q. Ou, Y. Wang, H. Wang, M. Yang, and M. Zhang. 2020. "The Precambrian Stratigraphic Sequence and Unconformities in Xingcheng Area of Liaoning Province, China, With Discussion of the Sedimentary-Paleogeographic Evolution of the Southeastern Yanshan Taphrogenic Trough Basin." *Acta Sedimentologica Sinica* 38: 687–711.

Li, Z., C. Wei, B. Chen, B. Fu, and M. Gong. 2020. "Late Neoarchean Reworking of the Mesoarchean Crustal Remnant in Northern Liaoning, North China Craton: A U-Pb-Hf-O-Nd Perspective." *Gondwana Research* 80: 350–369.

Liu, C., G. Zhao, F. Liu, J. Shi, and L. Ji. 2020. "Detrital Zircon Records of Late Paleoproterozoic to Early Neoproterozoic Northern North China Craton Drainage Reorganization: Implications for Supercontinent Cycles." *GSA Bulletin* 132: 2135–2153.

Liu, E., S. Chen, D. Yan, et al. 2022. "Detrital Zircon Geochronology and Heavy Mineral Composition Constraints on Provenance Evolution in the Western Pearl River Mouth Basin, Northern South China Sea: A Source to Sink Approach." *Marine and Petroleum Geology* 145: 105884.

Liu, X., J. Cai, and G. Yan. 2011. "Lithogeochemistry and Geochronology of Xiong'er Group Yanyaozhai Subvolcanics in the Southern Margin of the North China Craton and Their Geological Significance." *Acta Geologica Sinica* 85: 1134–1145.

Liu, X., H. Liu, P. Gao, W. Li, H. Liu, and J. Hou. 2021. "Detrital Zircon U-Pb-Hf Isotopes From the Yanliao Intracontinental Rift Sediments: Implications for Multiple Phases of Neoarchean-Paleoproterozoic Juvenile Crustal Growth in the North China Craton." *Gondwana Research* 96: 76–88.

Liu, X., J. Zhang, S. Li, X. Li, and C. Yin. 2020. "Tectono-Sedimentary Evolution of the Mesoproterozoic Basins in the Southern Yan-Liao and Mianchi-Queshan Areas: Insights From Stratigraphic Pattern and Detrital Zircon Geochronology." *International Journal of Earth Sciences* 109: 43–62.

Lu, L., J. Li, M. Yang, S. Yuan, and X. Bai. 2017. "Geochemistry Characteristics of the Diaoyutai Complexes in Liaoning, Eastern North China Craton." *Acta Geologica Sinica (English Edition)* 91: 164–165.

Lu, S. N., H. Li, H. M. Li, et al. 2003. "U-Pb Isotopie Ages and Their Significance of Alkaline Granite in the Souther Margin of the North China Craton." *Geological Bulletin of China* 22: 762–768.

Lu, S. N., and H. M. Li. 1991. "A Precise U-Pb Single Zircon Age Determination for the Volcanics of Dahongyu Formation, Changcheng System in the Jixian." *Bulletin of the Chinese Academy of Geological Science* 22: 137–146.

Lu, S., G. Zhao, H. Wang, and G. Hao. 2008. "Precambrian Metamorphic Basement and Sedimentary Cover of the North China Craton: A Review." *Precambrian Research* 160: 77–93.

Ludwig, K. R. 2012. *ISOPLOT 3.75 a Geochronological Toolkit for Microsoft Excel*. Berkeley Geochronology Centre Special Publication.

Meng, Q. R., H. H. Wei, Y. Q. Qu, and S. X. Ma. 2011. "Stratigraphic and Sedimentary Records of the Rift to Drift Evolution of the Northern North China Craton at the Paleo- to Mesoproterozoic Transition." *Gondwana Research* 20: 205–218.

Miao, L., M. Moczydłowska, S. Zhu, and M. Zhu. 2019. "New Record of Organic-Walled, Morphologically Distinct Microfossils From the Late Paleoproterozoic Changcheng Group in the Yanshan Range, North China." *Precambrian Research* 321: 172–198.

Mo, C., H. Liang, X. Wang, J. Cheng, and H. Li. 1997. "Zircon U-Pb Dating of Shuiquangou Alkaline Complex Intrusives, Northwestern Hebei Province." *Chinese Science Bulletin* 42: 772–775.

Pan, J., Y. Qu, R. Ma, Z. Pan, and H. Wang. 2013. "Sedimentary and Tectonic Evolution of the Meso-Neoproterozoic Strata in the Northern Margin of the North China Block." *Geological Journal of China Universities* 19: 109.

Pang, L., X. Zhu, B. Hu, W. Wang, Q. Sun, and T. Zhao. 2020. "Detrital Zircon U-Pb Age and hf Isotopic Composition and Whole-Rock Geochemical Characteristics of the Statherian Huangqikou Formation, Western Margin of the North China Craton: Implications for Provenance and Tectonic Evolution." *Precambrian Research* 347: 105840.

Paton, C., J. Hellstrom, B. Paul, J. Woodhead, and J. Hergt. 2011. "Iolite: Freeware for the Visualisation and Processing of Mass Spectrometric Data." *Journal of Analytical Atomic Spectrometry* 26: 2508.

Peng, P. 2015. "Precambrian Mafic Dyke Swarms in the North China Craton and Their Geological Implications." *Science China Earth Sciences* 58: 649–675.

Peng, P., W. Bleeker, R. E. Ernst, U. Söderlund, and V. McNicoll. 2011. "U–Pb baddeleyite ages, distribution and geochemistry of 925Ma mafic dykes and 900Ma sills in the North China craton: Evidence for a Neoproterozoic mantle plume." *Lithos* 127, no. 1–2: 210–221. https://doi.org/10.1016/j.lithos.2011.08.018.

Peng, P., F. Liu, M. Zhai, and J. Guo. 2012. "Age of the Miyun Dyke Swarm: Constraints on the Maximum Depositional Age of the Changcheng System." *Chinese Science Bulletin* 57: 105–110.

Peng, P., M. Zhai, R. E. Ernst, J. Guo, F. Liu, and B. Hu. 2008. "A 1.78 Ga Large Igneous Province in the North China Craton: The Xiong'er Volcanic Province and the North China Dyke Swarm." *Lithos* 101: 260–280.

Pourteau, A., M. A. Smit, Z.-X. Li, et al. 2018. "1.6 Ga Crustal Thickening Along the Final Nuna Suture." *Geology* 46: 959–962.

Qiao, X., L. Gao, and C. Zhang. 2007. "New Idea of the Meso-And Neoproterozoic Chronostratigraphic Chart and Tectonic Environmentin Sino-Korean Plate." *Geological Bulletin of China* 26: 503–509.

Qu, Y., Q. Meng, S. Ma, L. Li, and G. Wu. 2010. "Geological Characteristics of Unconformities in Mesoproterozoic Successions in the Northern Margin of North China Block and Their Tectonic Implication." *Earth Science Frontiers* 17: 112–127.

Qu, Y., J. Pan, L. Liang, Z. Yang, and H. Wang. 2012. "The Attributes of the Mesoproterozoic Unconformities in the Yanliao Rift Trough." *Sedimentary Geology and Tethyan Geology* 32: 11–22.

Ren, K., G. Yan, J. Cai, et al. 2006. "Chronology and Geological Implication of the Palco-Mesoproterozoic Alkaline-Rich Intrusions Belt From the Northern Part in the North China Craton." *Acta Petrologica Sinica* 22: 377–386.

Rubatto, D. 2017. "Zircon: The Metamorphic Mineral." *Reviews in Mineralogy and Geochemistry* 83: 261–295.

Santosh, M. 2010. "Assembling North China Craton Within the Columbia Supercontinent: The Role of Double-Sided Subduction." *Precambrian Research* 178: 149–167.

Santosh, M., P. Gao, B. Yu, C.-X. Yang, and S. Kwon. 2020. "Neoarchean Suprasubduction Zone Ophiolite Discovered From the Miyun Complex: Implications for Archean-Paleoproterozoic Wilson Cycle in the North China Craton." *Precambrian Research* 342: 105710.

Sharman, G. R., and M. A. Malkowski. 2020. "Needles in a Haystack: Detrital Zircon UPb Ages and the Maximum Depositional Age of Modern Global Sediment." *Earth-Science Reviews* 203: 103109.

Sharman, G. R., J. P. Sharman, and Z. Sylvester. 2018. "detritalPy: A Python-Based Toolset for Visualizing and Analysing Detrital Geo-Thermochronologic Data." *Depositional Record* 4: 202–215.

Sláma, J., J. Košler, D. J. Condon, et al. 2008. "Plešovice Zircon—A New Natural Reference Material for U–pb and hf Isotopic Microanalysis." *Chemical Geology* 249, no. 1: 1–35.

Sneed, E. D., and R. L. Folk. 1958. "Pebbles in the Lower Colorado River, Texas: A Study in Particle Morphogenesis." *Journal of Geology* 66: 114–150.

Song, B. 2015. "Shrimp Zircon U-Pb Age Measurement: Sample Preparation, Measurement, Data Processing and Explanation." *Geological Bulletin of China* 34: 1777–1788.

Spencer, C. J., C. L. Kirkland, and R. J. M. Taylor. 2016. "Strategies Towards Statistically Robust Interpretations of In Situ U–pb Zircon Geochronology." *Geoscience Frontiers* 7: 581–589.

Spencer, C. J., J. B. Murphy, C. L. Kirkland, Y. Liu, and R. N. Mitchell. 2018. "A Palaeoproterozoic Tectono-Magmatic Lull as a Potential Trigger for the Supercontinent Cycle." *Nature Geoscience* 11: 97–101.

Su, W., H. Li, W. D. Huff, et al. 2010. "Shrimp U-Pb Dating for a K-Bentonite Bed in the Tieling Formation, North China." *Chinese Science Bulletin* 55: 3312–3323.

Sun, S. L., Y. F. Li, T. Zhang, et al. 2021. "Biomarker Characteristics and Implication of the Mesoproterozoic Gaoyuzhuang Formation of Yanliao Rift Zone." *Geology and Resource* 30: 341–349.

Tan, C., Y. Lu, X. Li, et al. 2021. "Carbon, Oxygen and Strontium Isotopes of the Mesoproterozoic Jixian System (1.6-1.4 Ga) in the Southern Margin of the North China Craton and the Geological Implications." *International Geology Review* 63: 1951–1968.

Tapani Rämö, O., I. Haapala, M. Vaasjoki, J.-H. Yu, and H.-Q. Fu. 1995. "1700 Ma Shachang Complex, Northeast China: Proterozoic Rapakivi Granite Not Associated With Paleoproterozoic Orogenic Crust." *Geology* 23: 815–818.

Vermeesch, P. 2004. "How Many Grains Are Needed for a Provenance Study?" *Earth and Planetary Science Letters* 224: 441–451.

Vermeesch, P. 2013. "Multi-Sample Comparison of Detrital Age Distributions." *Chemical Geology* 341: 140–146.

Vermeesch, P. 2018. "Isoplotr: A Free and Open Toolbox for Geochronology." *Geoscience Frontiers* 9: 1479–1493.

Vermeesch, P. 2021. "Maximum Depositional Age Estimation Revisited." *Geoscience Frontiers* 12: 843–850.

Wan, Y., D. Liu, W. Wang, et al. 2011. "Provenance of Meso- to Neoproterozoic Cover Sediments at the Ming Tombs, Beijing, North China Craton: An Integrated Study of U–pb Dating and hf Isotopic Measurement of Detrital Zircons and Whole-Rock Geochemistry." *Gondwana Research* 20: 219–242.

Wang, C., P. Peng, X. Wang, Q. Li, X. Xu, and S. Yang. 2016. "The Generations and U-Pb Dating of Baddeleyites from the Taihang Dyke Swarm in North China and Their Implications for Magmatic Evolution." *Acta Petrologica Sinica* 32: 646–658.

Wang, Q., H. Yang, D. Yang, and W. Xu. 2014. "Mid-Mesoproterozoic (~1.32ga) Diabase Swarms from the Western Liaoning Region in the Northern Margin of the North China Craton: Baddeleyite Pb–Pb Geochronology, Geochemistry and Implications for the Final Breakup of the Columbia Supercontinent." *Precambrian Research* 254: 114–128.

Wang, W., S. Liu, X. Bai, et al. 2013. "Geochemistry and Zircon U–Pb–Hf Isotopes of the Late Paleoproterozoic Jianping Diorite–Monzonite–Syenite Suite of the North China Craton: Implications for Petrogenesis and Geodynamic Setting." *Lithos* 162–163: 175–194.

Wang, W., S. Liu, M. Santosh, et al. 2015. "Late Paleoproterozoic Geodynamics of the North China Craton: Geochemical and Zircon U–pb–hf Records From a Volcanic Suite in the Yanliao Rift." *Gondwana Research* 27: 300–325.

Weltje, G. J., and H. von Eynatten. 2004. "Quantitative Provenance Analysis of Sediments: Review and Outlook." *Sedimentary Geology* 171: 1–11.

Wiedenbeck, M., J. Hanchar, W. Peck, et al. 2004. "Further Characterisation of the 91500 Zircon Crystal." *Geostandards and Geoanalytical Research* 28: 9–39.

Yang, J., F. Wu, X. Liu, and L. Xie. 2005. "Zircon U-Pb Ages and hf Isotopes and Their Geological Significance of the Miyun Rapakivi Granites From Beijing, China." *Acta Petrologica Sinica* 21: 1633–1644.

Yonkee, W. A., and A. B. Weil. 2015. "Tectonic Evolution of the Sevier and Laramide Belts Within the North American Cordillera Orogenic System." *Earth-Science Reviews* 150: 531–593.

Zhai, M., B. Hu, P. Peng, and T. Zhao. 2014. "Meso-Neoproterozoic Magmatic Events and Multi-Stage Rifting in the NCC." *Earth Science Frontiers* 21: 100–119.

Zhai, M., B. Hu, T. Zhao, P. Peng, and Q. Meng. 2015. "Late Paleoproterozoic-Neoproterozoic multi-rifting events in the North China Craton and their geological significance: A study advance and review." *Tectonophysics* 662: 153–166. https://doi.org/10.1016/j.tecto.2015.01.019.

Zhai, M., T. Li, P. Peng, B. Hu, F. Liu, and Y. Zhang. 2010. "Precambrian Key Tectonic Events and Evolution of the North China Craton." *Geological Society, London, Special Publications* 338: 235–262.

Zhai, M., and W. Liu. 2003. "Palaeoproterozoic Tectonic History of the North China Craton: A Review." *Precambrian Research* 122: 183–199.

Zhai, M., and M. Santosh. 2013. "Metallogeny of the North China Craton: Link With Secular Changes in the Evolving Earth." *Gondwana Research* 24: 275–297.

Zhai, M. G., J. A. Shao, J. Hao, and P. Peng. 2003. "Geological Signature and Possible Position of the North China Block in the Supercontinent Rodinia." *Gondwana Research* 6: 171–183.

Zhang, J., H. Tian, H. K. Li, et al. 2015. "Age, Geochemistry and Zircon hf Isotope of the Alkaline Basaltic Rocks in the Middle Section of the Yan-Liao Aulacogen Along the Northern Margin of the North China Craton: New Evidence for the Breakup of the Columbia Supercontinent." *Acta Petrologica Sinica* 31: 3129–3146.

Zhang, S. H., R. E. Ernst, T. J. Munson, et al. 2022. "Comparisons of the Paleo-Mesoproterozoic Large Igneous Provinces and Black Shales in the North China and North Australian Cratons." *Fundamental Research* 2: 84–100.

Zhang, S., S. Liu, Y. Zhao, J. Yang, B. Song, and X. Liu. 2007. "The 1.75–1.68ga Anorthosite-Mangerite-Alkali Granitoid-Rapakivi Granite Suite from the Northern North China Craton: Magmatism Related to a Paleoproterozoic Orogen." *Precambrian Research* 155: 287–312.

Zhang, S., B. Zhang, L. Bian, Z. Jin, D. Wang, and J. Chen. 2007. "The Xiamaling Oil Shale Generated Through Rhodophyta Over 800 Ma Ago." *Science in China Series D: Earth Sciences* 50: 527–535.

Zhang, S., Y. Zhao, X. Li, R. E. Ernst, and Z. Yang. 2017. "The 1.33–1.30 Ga Yanliao Large Igneous Province in the North China Craton: Implications for Reconstruction of the Nuna (Columbia) Supercontinent, and Specifically with the North Australian Craton." *Earth and Planetary Science Letters* 465: 112–125.

Zhang, S., Y. Zhao, H. Ye, K. Hou, and C. Li. 2012. "Early Mesozoic Alkaline Complexes in the Northern North China Craton: Implications for Cratonic Lithospheric Destruction." *Lithos* 155: 1–18.

Zhang, S., Y. Zhao, H. Ye, and G. Hu. 2016. "Early Neoproterozoic Emplacement of the Diabase Sill Swarms in the Liaodong Peninsula and Pre-Magmatic Uplift of the Southeastern North China Craton." *Precambrian Research* 272: 203–225.

Zhang, S. H., Y. Zhao, H. Ye, J. M. Hu, and F. Wu. 2013. "New Constraints on Ages of the Chuanlinggou and Tuanshanzi Formations of the Changcheng System in the Yan-Liao Area in the Northern North China Craton." *Acta Petrologica Sinica* 29: 2481–2490.

Zhang, W., F. Liu, and C. Liu. 2021. "Provenance Transition From the North China Craton to the Grenvillian Orogeny-Related Source: Evidence From Late Mesoproterozoic-Early Neoproterozoic Strata in the Liao-Ji Area." *Precambrian Research* 362: 106281.

Zhao, G., M. Sun, S. A. Wilde, and S. Z. Li. 2005. "Late Archean to Paleoproterozoic Evolution of the North China Craton: Key Issues Revisited." *Precambrian Research* 136: 177–202.

Zhao, T., F. Chen, M. Zhai, and B. Xia. 2004. "Single Zircon U-Pb Ages and Their Geological Significance of the Damiao Anorthosite Complex, Hebei Province, China." *Acta Petrologica Sinica* 20: 685–690.

Zheng, X. C. 2016. "The Geochemical Characteristics of Siliceous Rocks in Mesoproterozoic Erathem in Chicheng Area of Yanshan Belt." *Journal of Oli and Gas Technology* 38: 16–22.

Zheng, Y. F., W.-J. Xiao, and G. Zhao. 2013. "Introduction to Tectonics of China." *Gondwana Research* 23: 1189–1206.

Zhu, S., H. Li, L. Sun, and H. Liu. 2022. "Meso-Neoproterozoic Stratigraphic Sequences in the Yanliao Faulted-Depression Zone, North China Craton." In *Meso-Neoproterozoic Geology and Petroleum Resources in China*, edited by S. Zhu, H. Li, L. Sun, and H. Liu, 47–89. Springer.

Supporting Information

Additional supporting information can be found online in the Supporting Information section. **Data S1:** bre70068-sup-0001-Supinfo1.docx. **Data S2:** bre70068-sup-0002-DataS1.xlsx. **Data S3:** bre70068-sup-0003-DataS2.xlsx. **Data S4:** bre70068-sup-0004-DataS3.xlsx.